https://doi.org/10.5194/acp-2019-633
Preprint. Discussion started: 30 September 2019

Atmospheric Chemistry and Physics Discussions

Distinct diurnal variation of organic aerosol hygroscopicity and its relationship with oxygenated organic aerosol

Ye Kuang[1,*,†], Yao He[2,†], Wanyun Xu[5], Yele Sun[2,*], Pusheng Zhao[6], Yafang Cheng[4], Gang Zhao[3], Jiangchuan Tao[1], Nan Ma[1], Hang Su[4], Yanyan Zhang[1], Jiayin Sun[7], Peng Cheng[7], Wenda Yang[7], Shaobin Zhang[1], Cheng Wu[7], Chunsheng Zhao[3]

[1]{Institute for Environmental and Climate Research, Jinan University, Guangzhou 511443, China}

[2] {State Key Laboratory of Atmospheric Boundary Layer Physics and Atmospheric Chemistry, Institute of Atmospheric Physics, Chinese Academy of Sciences, Beijing, China}

[3] {Department of Atmospheric and Oceanic Sciences, School of Physics, Peking University, Beijing, China}

[4] {Max Planck Institute for Chemistry, Mainz 55128, Germany}

[5] {State Key Laboratory of Severe Weather & Key Laboratory for Atmospheric Chemistry, Institute of Atmospheric Composition, Chinese Academy of Meteorological Sciences, Beijing, 100081, China}

[6] {Institute of Urban Meteorology, China Meteorological Administration, Beijing, 100089, China}

[7] {Institute of Mass Spectrometer and Atmospheric Environment, Jinan University, Guangzhou 510632, China}

† These authors contribute equally to this paper.

*Correspondence to: Ye Kuang (kuangye@jnu.edu.cn), Yele Sun (sunyele@mail.iap.ac.cn)

https://doi.org/10.5194/acp-2019-633
Preprint. Discussion started: 30 September 2019

Atmospheric Chemistry and Physics Discussions

Abstract

The hygroscopicity of organic aerosols (OA) is important for investigation of its climatic and environmental impacts. However, the hygroscopicity parameter κ_{Org} remains poorly characterized, especially in the relatively polluted environment on the North China Plain (NCP). Here we conducted simultaneous wintertime measurements of bulk aerosol chemical compositions of $PM_{2.5}$ and PM_1 and bulk aerosol hygroscopicity of PM_{10} and PM_1 on the NCP using a capture vaporizer time-of-flight aerosol chemical speciation monitor (ToF-ACSM) and a humidified nephelometer system which measures aerosol light scattering enhancement factor $f(\mathrm{RH})$. A method for calculating κ_{Org} based on $f(\mathrm{RH})$ and bulk aerosol chemical composition measurements was developed. We found that κ_{Org} varied in a wide range with significant diurnal variations. The derived κ_{Org} ranged from almost 0.0 to 0.25 with an average (±1σ) of 0.08 (±0.06) for the entire study. The derived κ_{Org} was highly correlated with f_{44} (fraction of *m/z* 44 in OA), an indicator of oxidation degree of OA (R=0.79), and the relationship can be parameterized as $\kappa_{Org} = 1.04 \times f_{44}$ - 0.02. On average, κ_{Org} reached the minimum (0.02) in the morning near 07:30 and then increased rapidly reaching the peak value of 0.16 near 14:30. The diurnal variations of κ_{Org} were highly and positively correlated with those of mass fractions of oxygenated OA (R = 0.95), indicating that photochemical processing played a dominant role for the increase of κ_{Org} in winter on NCP. Results in this study demonstrate the potential wide applications of humidified nephelometer system together with aerosol composition measurements for investigating the hygroscopicity of OA in various environments, and highlight that the parameterization of κ_{Org} as a function of OA aging processes needs to be considered in chemical transport models for better evaluating the impacts of OA on cloud formation, atmospheric chemistry and radiative forcing.

1 Introduction

Aerosol hygroscopic growth plays significant roles in different atmospheric processes including atmospheric radiation transfer, cloud formation, visibility degradation, atmospheric multiphase chemistry and even air pollution health effects, and therefore is crucial for studies on aerosol climatic and environmental impacts. Organic materials in ambient aerosol particles, usually referred to as

https://doi.org/10.5194/acp-2019-633
Preprint. Discussion started: 30 September 2019

Atmospheric Chemistry and Physics Discussions

organic aerosol (OA), contribute substantially to ambient aerosol mass and frequently contribute more than half to submicron aerosol particles mass under dry state (Jimenez et al., 2009). The hygroscopicity parameter κ (Petters and Kreidenweis, 2007) of organic aerosols (κ_{Org}) is a key parameter for investigating the roles of organic aerosol in radiative forcing, cloud formation and atmospheric chemistry. Liu and Wang (2010) demonstrated that ±50% changes in κ of secondary organic aerosol (0.14±0.07) can lead to 40% changes in predicted cloud condensation nuclei (CCN) concentration. Rastak et al. (2017) reported a global average difference in aerosol radiative forcing of -1 W/m^2 between κ_{Org} of 0.05 and 0.15, which shares the same order with the overall climate forcing of anthropogenic aerosol particles during the industrialization period. Li et al. (2019) reported that organic aerosol liquid water contributed 18-32% to total particle liquid water content in Beijing. Despite its importance, κ_{Org} has not yet been well characterized due to the extremely complex chemical compositions of organic aerosol. Therefore, it is important to conduct more researches on the spatiotemporal variation and size dependence of κ_{Org} and its relationship with aerosol chemical compositions to reach a better characterization and come up with more appropriate parameterization schemes in chemical, meteorological and climate models.

The large variety in OA chemical constituents makes it difficult to directly link κ_{Org} to specific organic aerosol compositions. The OA chemical composition is tightly connected to their volatile organic precursors, which are also rich in variety and come from many natural and anthropogenic sources. OA with different oxidation levels will also behave differently in respect to hygroscopic growth. Thus, studies on κ_{Org} at different locations and time periods have reported distinct characteristics. Many studies have investigated the influence of OA oxidation level (represented by O:C ratio or fraction of m/z 44 ACSM ion signal, f_{44}) on its hygroscopicity (Chang et al., 2010;Lambe et al., 2011;Duplissy et al., 2011;Mei et al., 2013b;Wu et al., 2013;Hong et al., 2015;Chen et al., 2017;Massoli et al., 2010) and have reached a conclusion that in average κ_{Org} generally increases as a function of organic aerosol oxidation level, however, the statistical empirical relationship between κ_{Org} and O:C ratio or f_{44} differs much among different studies. Several studies have also analyzed the diurnal variation characteristics of κ_{Org} at different locations and periods (Cerully et al., 2015;Bougiatioti et al., 2016;Deng et al., 2018;Deng et al., 2019;Thalman et al., 2017), with some exhibiting distinct diurnal variations (Deng et al., 2018;Deng et al., 2019;Bougiatioti et al., 2016) and

https://doi.org/10.5194/acp-2019-633
Preprint. Discussion started: 30 September 2019


Atmospheric Chemistry and Physics Discussions

others not so much (Cerully et al., 2015). Studies on κ_{Org} has already been reported for several locations around the world, however, only Wu et al. (2016) have reported the influences of OA oxidation level on κ_{Org} in the North China Plain (NCP) region, which is one of the most polluted regions on earth. The diurnal characteristics of κ_{Org} in the NCP have not been reported so far. Therefore, more investigation into the diurnal variation of κ_{Org} and its relationship to OA oxidation level is required to better understand its characteristics in the NCP.

In addition, in previous studies on κ_{Org}, the Humidity Tandem Differential Mobility Analyzer (HTDMA) or CCN counter were applied for aerosol hygroscopicity measurements. Both the HTMDA and size-resolved CCN measurements can only be used to derive a κ within a certain size range (HDTMA: usually diameter below 300 nm, with a reported highest diameter of 360 nm (Deng et al., 2019), CCN: with diameter up to ~200 nm (Zhang et al., 2014;Rose et al., 2010)). The aerosol particles contributing most to aerosol optical properties (Bergin et al., 2001;Quinn et al., 2002;Cheng et al., 2008;Ma et al., 2011;Kuang et al., 2018) and aerosol liquid water contents (Bian et al., 2014) in continental regions are usually in the diameter range of 200 nm to 1μm, which the HTDMA and CCN hygroscopicity measurements cannot represent. Results from several studies have reported that κ_{Org} usually differentiates among particle size (Frosch et al., 2011;Kawana et al., 2016;Deng et al., 2019). Especially, results from Deng et al. (2019) demonstrated that κ_{Org} increase with the increase in particle dry diameter. These results further demonstrate that studies about information of κ_{Org} of larger particles would be helpful for κ_{Org} studies.

Other than HTDMA and CCN counter, the humidified nephelometer system which measures aerosol light scattering enhancement factors is also widely used in aerosol hygroscopicity research (Titos et al., 2016). The hygroscopicity parameter κ retrieved from measured light scattering enhancement factor is usually referred to as $\kappa_{f(\mathrm{RH})}$ (Chen et al., 2014;Kuang et al., 2017), which represents the overall hygroscopicity of aerosol particles with their diameters ranging from 200 nm to 800 nm for continental aerosols (see discussions in Sect.3.3 for physical understanding of $\kappa_{f(\mathrm{RH})}$). Using the retrieved $\kappa_{f(\mathrm{RH})}$ together with the according bulk aerosol chemical compositions measurements of PM_1 (particulate matter with aerodynamic diameter less than 1 μm, corresponding to mobility diameter of about 800 nm), κ_{Org} can be derived, representing the hygroscopicity of organic aerosol particles in the diameter range of 200 to 800 nm. In this study, both the light scattering enhancement factor of PM_{10} (particulate matter with aerodynamic diameter less than 10 μm) and PM_1

https://doi.org/10.5194/acp-2019-633
Preprint. Discussion started: 30 September 2019

Atmospheric Chemistry and Physics Discussions

particles were measured. The aerosol chemical compositions were measured using an aerosol chemical speciation monitor (ACSM). With these two aspects of aerosol measurements, κ_{Org} is derived, and the relationship between κ_{Org} and the OA oxidation degree, as well as the diurnal variation of κ_{Org} are investigated.

Site and instrument information are introduced in Sect.2. Method of deriving κ_{Org} based on retrieved $\kappa_{f(\mathrm{RH})}$ and bulk aerosol chemical compositions measurements are proposed and discussed in Sect.3. Results and discussions are presented in Sect.4, followed by conclusions.

2 Site and instruments

From 11th November to 24th December 2018, continuous measurements of physical, optical and chemical properties of ambient aerosol particles as well as meteorological parameters such as temperature, wind speed and direction and relative humidity were made at the Gucheng site in Dingxing county, Hebei province, China. This site is an Ecological and Agricultural Meteorology Station (39°09'N, 115°44'E) of the Chinese Academy of Meteorological Sciences. The site locates between Beijing (~ 100km) and Baoding (~40km), two large cities on the North China Plain, and is surrounded by farmland and small residential towns.

2.1 Inlet system and instruments

During this field campaign, all instruments were housed in an air-conditioned container, with the temperature held almost constant near 24 ℃. The schematic diagram of the inlet systems for the aerosol sampling instruments is displayed in Fig.1. Three inlet impactors are used for aerosol sampling, two PM_{10} inlets and one PM_1 inlet, respectively sampling ambient aerosol particles with aerodynamic diameter less than 10 μm and 1 μm. Nafion driers with lengths of 1.2 m were placed downstream of each PM impactor inlet, which can drop the RH of sampled air below 15%, thus, sampled aerosol particles can be treated as in dry state. Additionally, downstream every PM impactor inlet an MFC (mass flow controller) and a pump was added for automatic flow compensation, to ensure that each impactor reaches their required flow rate of 16.7 L/min and guaranteeing for the right cut diameters.

https://doi.org/10.5194/acp-2019-633
Preprint. Discussion started: 30 September 2019

Atmospheric Chemistry and Physics Discussions

Aerosol sampling instruments can be categorized into four groups according to their inlet routes. The first group (group1) downstream of the first PM10 inlet is comprised of only one instrument, the Aerodynamic Particle Sizer (APS, TSI Inc., Model 3321), measuring the size distribution of ambient aerosol particles with aerodynamic diameter ranging from 700 nm to 20 μm at a temporal resolution of 20 seconds. The second group (group 2) includes a humidified nephelometer system (consisting of two nephelometers and a humidifier) that measures aerosol optical properties (scattering and back

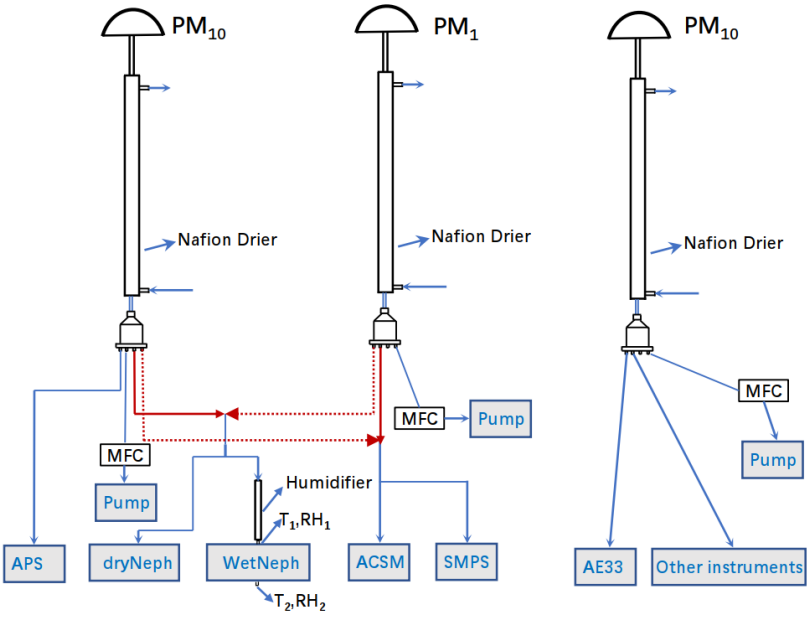

Figure 1. Schematic diagram of the inlet systems for aerosol sampling instruments

scattering coefficients at three wavelengths: 450 nm, 525 nm, 635 nm) of ambient aerosol particles in dry state (DryNeph) and under 85% RH condition (WetNeph). The third group (group3) includes two instruments, an ACSM and a scanning mobility particle sizer (SMPS; TSI model 3080). The ACSM measures non-refractory particulate matter (NR-PM) species including organics, SO_4^{2-}, NO_3^-, NH_4^+, and Cl^- with an air flow of 0.1 L/min and a time resolution of 2 minutes. Since the ACSM` instrument comes with an $PM_{2.5}$ impactor, chemical composition of $PM_{2.5}$ rather than of PM_{10} were measured.

The SMPS measures particle mobility diameter size distributions with a diameter range of 12 nm to 760 nm. The inlets of group2 and group3 switches every 15 minutes, as denoted by the dashed and solid red lines in Fig.1, enabling the instruments of these two groups to alternately measure the chemical and optical properties of PM_{10} and PM_1. The fourth group (group4) includes an AE33

https://doi.org/10.5194/acp-2019-633
Preprint. Discussion started: 30 September 2019

Atmospheric Chemistry and Physics Discussions

aethalometer (Drinovec et al., 2015) and other aerosol instruments. Due to technical issues with the humidifier, the humified nephelometer system started to operate continuously since the 30th Nov .

In addition, the ambient meteorological parameters like RH, temperature, wind speed and direction and air pressure were observed using an automatic weather station at a 1 minute time resolution.

2.2 The humidified nephelometer system

The humidified nephelometer system we built was set up to measure dry state aerosol optical properties at a fixed RH of 85%. The RH of the air sample is increased by a humidifier that consists of two layers. The inner layer is a Gore-Tex tube layer passing through sampled air, while the outer layer is a stainless-steel tube with circulating liquid water. The water vapor penetrates through the Gore-Tex tube and humidifies the sample air, while liquid water is kept from the inner layer by the Gore-Tex material. Upon the switch of inlets between group 2 and group 3, delays in valve switching caused instantaneous low pressure in the sample air, which broke the humidifier with the Gore-Tex tube after four days of continuous operation (3th, Dec) and flooded the WetNeph. The WetNeph was fixed and recalibrated and a commercial Nafion drier (60 cm long, Perma Pure company) replaced the Gore-Tex tube, which works the same way but is more resistant to low pressure. The temperature of the circulating water layer is controlled by a water bath and specified by an algorithm that adjusts the water temperature to maintain a relatively constant RH in the sensing volume of the WetNeph. To monitor the RH in the sensing volume of the WetNeph, two temperature and RH sensors (Vaisala HMP110, with accuracies of ± 0.2 ℃ and ± 1.7 % for RH between 0 to 90%, respectively, and ± 2.5 % for RH between 90 to 100%) were placed at the inlet and outlet of the WetNeph. Defining measured RHs and temperatures at the inlet and outlet of the WetNeph as RH_1/T_1 and RH_2/T_2, the according dew point temperatures T_{d1} and T_{d2} can be calculated and the average value $\overline{T_d}$ was treated as the dew point of the sample air in the sensing volume of WetNeph. The sample RH is calculated using $\overline{T_d}$ and the sample temperature measured by a sensor inside the sample cavity of the nephelometer.

https://doi.org/10.5194/acp-2019-633
Preprint. Discussion started: 30 September 2019

Atmospheric Chemistry and Physics Discussions

2.3 ACSM measurements and data analysis

The mass concentration and chemical composition of NR-PM species were measured with the Aerodyne ToF-ACSM which is equipped with a $PM_{2.5}$ aerodynamic lens (Williams et al., 2010) and a novel capture vaporizer (CV) (Xu et al., 2017;Hu et al., 2017) to extend the measured particle size to 2.5 μm. Detailed instrument descriptions were given in Fröhlich et al. (2013) and Xu et al. (2017). The ToF-ACSM data were analyzed with the standard data analysis software (Tofware v2.5.13, https://sites.google.com/site/ariacsm/) within Igor Pro (v6.37, WaveMetrics, Inc., Oregon, USA). A collection efficiency (CE) of 1 was used for all aerosol species, because the capture vaporizer has been proven to reach a unit CE for ambient aerosols (Hu et al., 2017;Hu et al., 2018b). Relative ionization efficiencies (RIE) of 3.06 and 1.09 were used for ammonium and sulfate quantification respectively, and the default values of 1.1 and 1.4 were used for nitrate and organic aerosol (OA) respectively. Compared with the AMS with standard vaporizer, the CV-ToF-ACSM reports higher fragments at small *m/z*'s due to additional thermal decomposition associated with increased residence time and hot surface collisions (Hu et al., 2018a). As a result, f_{44} from CV-ToF-ACSM measurements is often much higher than those previously reported from AMS, yet they are well correlated (Hu et al., 2018a).

The organic mass spectra from *m/z* 12 to 214 were analyzed by positive matrix factorization (PMF) (Paatero and Tapper, 1994) with an Igor Pro based PMF evaluation tool (v3.04) (Ulbrich et al., 2009). The *m/z's* of 38, 49, 63 and 66 were removed from both PM_1 and $PM_{2.5}$ PMF inputs considering their small contributions to the total organic signal and their high noise. The PMF results were then evaluated following the procedures detailed in Zhang et al. (2011). After carefully evaluating the mass spectral profiles, diurnal patterns and temporal variation of the OA factors and comparing them with other collocated measurements, a five-factor solution was selected for both PM_1 and $PM_{2.5}$. The five factors include four primary factors, i.e., hydrocarbon-like OA (HOA), cooking OA (COA), biomass burning OA (BBOA), and coal combustion OA (CCOA), and a secondary factor, oxygenated OA (OOA). More detailed descriptions on the PMF results will be given in He et al. (in preparation).

2.4 Data reprocessing

The size distributions measured by APS were converted to mobility-equivalent size distributions using spherical shape assumptions and an effective particle density of 1.7 g/cm^3. Note that the

https://doi.org/10.5194/acp-2019-633
Preprint. Discussion started: 30 September 2019


Atmospheric Chemistry and Physics Discussions

designations of PM_{10} and PM_1 are in respect to aerosol aerodynamic diameters, while the corresponding mobility-equivalent cut diameters of the two impactors are approximately 7669 nm and 767 nm, respectively. For simplicity and consistency, we will continue to refer to them as the PM_{10} and PM_1 based on their aerodynamic diameter. For the case of PM_1 measurements, the mobility-equivalent cut diameter is quite near the upper range of the SMPS size range. Considering that the cut diameter of the impactor corresponds to the diameter of aerosol particles in ambient state (aerosol hygroscopic growth effect needs to be taken into account) and the SMPS measures the size distributions of aerosol particles in dry state, the SMPS measurements should be able to cover the full size range of PM_1. When the SMPS was sampling aerosol particles of PM_{10}, the size distributions measured by SMPS and APS was merged together and truncated to an upper limit of 7669 nm to provide full range particle number size distributions (PNSD). In addition, the AE33 measures aerosol absorption coefficient at several wavelengths, the mass concentrations of black carbon (BC) were converted from measured aerosol absorption coefficients at 880 nm with a mass absorption coefficient of 7.77 m^2/g (Drinovec et al., 2015).

Since group 2 and 3 switched between PM_1 and PM_{10} inlets every 15 minutes, all measurements were averaged over each 15 minute observation episode, resulting in valid time resolutions of 15 minutes for APS and BC PM_{10} measurements and 30 minutes for SMPS, ACSM and the humidified nephelometer system PM_1 and PM_{10} measurements, respectively. This resulted in a 15-minute time lag between the averaged datasets of group 2 and group 3. To match the time of all the measurement data, the measurements of SMPS, ACSM and the humidified nephelometer system were linearly interpolated to the 15-minute time resolution of the APS data.

3 Methodology

3.1 Calculations of hygroscopicity parameters κ_{sca} and κ from measurements of the humidified nephelometer system

The humidified nephelometer system measures aerosol light scattering coefficients and backscattering coefficients at three wavelengths under dry state and 85% RH condition, providing measurements of the light scattering enhancement factor $f(\mathrm{RH},\lambda)$, which is defined as

https://doi.org/10.5194/acp-2019-633
Preprint. Discussion started: 30 September 2019

Atmospheric Chemistry and Physics Discussions

$f(\mathrm{RH}=85\%,\lambda)=\frac{\sigma_{sp}(RH,\ \lambda)}{\sigma_{sp}(dry\ \lambda)}$, with λ being the light wavelength. In this study, we only calculate $f(\mathrm{RH},525\ \mathrm{nm})$ and refer to it hereinafter as $f(\mathrm{RH})$ for simplicity. Brock et al. (2016) proposed a single parameter formula to describe $f(\mathrm{RH},\lambda)$ as a function of RH. Kuang et al. (2017) further developed this parameterization scheme to better describe measured $f(\mathrm{RH})$ by including the reference RH (RH_0) in the dry nephelometer as shown in Eq.1, using which the optical hygroscopicity parameter κ_{sca} can be derived from $f(\mathrm{RH})_{measured}$.

$$f(\mathrm{RH})_{measured}=(1+\kappa_{sca}\frac{RH}{100-RH})/(1+\kappa_{sca}\frac{RH_0}{100-RH_0}) \quad (1)$$

An overall hygroscopicity parameter κ referred to as $\kappa_{f(\mathrm{RH})}$ can be retrieved from measured $f(\mathrm{RH})$ with the addition of simultaneously measured particle number size distribution (PNSD) and BC mass concentration (Chen et al., 2014;Kuang et al., 2017). The idea is to conduct an iterative calculation using the Mie theory and the κ-Köhler theory together to find a $\kappa_{f(\mathrm{RH})}$ that closes the gap between the simulated and the measured $f(\mathrm{RH})$. Details on the calculations of $\kappa_{f(\mathrm{RH})}$ can be found in Kuang et al. (2017).

3.2 Calculations of κ_{chem} from aerosol chemical composition measurements

For the calculation of aerosol hygroscopicity parameter κ based on measured chemical composition data (κ_{chem}), detailed information on the chemical species are needed. The ACSM can only provide bulk mass concentrations of SO_4^{2-}, NO_3^-, NH_4^+, Cl^- ions and organic components. For the inorganic ions, a simplified ion pairing scheme (as listed in Tab.1) was used to convert ion mass concentrations to mass concentrations of corresponding inorganic salts (Gysel et al., 2007;Wu et al., 2016).

Table 1. Densities (ρ) and hygroscopicity parameters (κ) of inorganic salts used in this study

Species	NH_4NO_3	NH_4HSO_4	$(NH_4)_2SO_4$	NH_4Cl
ρ (g cm^{-3})	1.72	1.78	1.769	1.527
κ	0.58	0.56	0.48	0.93

Mass concentrations of SO_4^{2-}, NO_3^-, NH_4^+, Cl^- are thus specified into ammonium sulfate (AS), ammonium nitrate (AN) ammonium chloride (AC) and ammonium bisulfate (ABS), with the κ values of these salts specified according to (Wu et al., 2016) and Liu et al. (2014) (Tab.1). For a given internal

https://doi.org/10.5194/acp-2019-633
Preprint. Discussion started: 30 September 2019

Atmospheric Chemistry and Physics Discussions

mixture of different aerosol chemical species, a simple mixing rule called Zdanovskii–Stokes–Robinson (ZSR) can be used for predicting the overall $\boldsymbol{\kappa_{chem}}$ on the basis of volume fractions of different chemical species (ε_i) (Petters and Kreidenweis, 2007):

$$\kappa_{chem} = \sum_i \kappa_i \cdot \varepsilon_i \qquad (2)$$

where κ_i and ε_i represent the hygroscopicity parameter κ and volume fraction of chemical component *i* in the mixture. Based on Eq.2, κ_{chem} can be calculated as follows:

$$\kappa_{chem} = \kappa_{AS}\varepsilon_{AS} + \kappa_{AN}\varepsilon_{AN} + \kappa_{ABS}\varepsilon_{ABS} + \kappa_{AC}\varepsilon_{AC} + \kappa_{BC}\varepsilon_{BC} + \kappa_{Org}\varepsilon_{Org} \qquad (3)$$

where κ_{Org} and ε_{Org} represent κ and volume fraction of total organics. Since black carbon is hydrophilic, κ_{BC} is assumed to be zero. With known $\boldsymbol{\kappa_{chem}}$, κ_{Org} can be calculated using the following formula:

$$\kappa_{Org} = \frac{\kappa_{chem} - (\kappa_{AS}\varepsilon_{AS} + \kappa_{AN}\varepsilon_{AN} + \kappa_{ABS}\varepsilon_{ABS} + \kappa_{AC}\varepsilon_{AC})}{\varepsilon_{Org}} \qquad (4)$$

To calculate volume fractions of individual species, their volume concentrations and the total volume concentration of aerosol particles (V_{tot}) are required. The volume concentration of salts can be calculated from the additive ion mass concentrations divided by their densities listed in Tab.1. The volume concentration of organics was calculated by assuming density of POA as 1 g/cm^3 and density of OOA as 1.4 g/cm^3 (Wu et al., 2016). For the calculation of V_{tot}, we have three choices. The first choice is to sum up the volume concentrations of all chemical species (AS, AN, ABS, AC, BC and organics), where the volume concentration of BC was calculated by assuming a density of 1.7 g/cm^3. We refer the calculated total volume concentration of aerosol particles to as $V_{tot,Chem}$. The second choice is to integrate V_{tot} from measured PNSD, using the equation $V_{tot,PNSD} = \int \frac{4}{3}\pi r^3 n(r) dr$, where r is the particle radius and n(r) is the measured PNSD. The third choice is to use the trained machine learning estimator to estimate the V_{tot} based on measurements of the dry nephelometer ($V_{tot,Neph}$) as was introduced in Kuang et al. (2018). V_{tot} of PM_1 calculated using these three methods were compared to each other and shown in Fig.S2. $V_{tot,Chem}$ correlates well with $V_{tot,PNSD}$, but in is on average 30% lower than that of $V_{tot,PNSD}$. Chemical components within aerosol particles such as dust, sea salt as well as metal ions could not be identified by ACSM. Since the Gucheng site is far from the ocean, sea salt should have negligible impacts on the total mass of PM_1. However, mineral dust

https://doi.org/10.5194/acp-2019-633
Preprint. Discussion started: 30 September 2019

Atmospheric Chemistry and Physics Discussions

can extend into the submicron range (Shao et al., 2007), which might be the cause for the underestimate in total mass concentration calculated using ACSM and BC data. $V_{tot,Neph}$ also correlates well with $V_{tot,PNSD}$, but is on average 16% lower than that of $V_{tot,PNSD}$. Closure studies between modelled and measured σ_{sp} and σ_{bsp} at 525 nm for PM_1 and PM_{10} aerosol particles all showed good agreement between theoretical modelling results and measurements (Fig.S1), with most points falling between the 20% relative deviation lines. However, modelled σ_{sp} for both PM_1 and PM_{10} were obviously higher than measured σ_{sp}, with an average relative difference of 22% and 13% between them for PM10 and PM1, respectively. The result for PM_1 explains why $V_{tot,Neph}$ was lower than $V_{tot,PNSD}$. Two reasons might have contributed to this discrepancy: (1) both PNSD and aerosol optical property measurements carry non-negligible uncertainties, with the SMPS bearing measurement uncertainty of 30% for particles larger than 200 nm, which contribute most to V_{tot} (Wiedensohler et al., 2012), and the nephelometer measured σ_{sp} having an uncertainty of 9% (Sherman et al., 2015;Titos et al., 2016); (2) The sampling tube length, valves, tube angles and flow rates are different for the dry nephelometer and SMPS (e.g. the tube length is much shorter and flow rate smaller for SMPS than those for the dry nephelometer), leading to different wall loss and loss in semi-volatile of aerosol components. ACSM and the dry nephelometer had similar tube length and nephelometer measurements bears less uncertainty than SMPS. Thus, $V_{tot,Neph}$ was chosen as V_{tot} in the calculations of Eq.4. Based on the calculated V_{tot}, the material unidentified by ACSM accounts for 19% of V_{tot} on average, could not be neglected in the κ_{Org} calculation. Thus, Eq.4 was modified as follows:

$$\kappa_{Org} = \frac{\kappa_{chem} - (\kappa_{AS} \cdot \varepsilon_{AS} + \kappa_{AN} \cdot \varepsilon_{AN} + \kappa_{ABS} \cdot \varepsilon_{ABS} + \kappa_X \cdot \varepsilon_X)}{\varepsilon_{Org}} \quad (5)$$

where κ_X and ε_X are hygroscopicity parameter κ and volume fractions of the unidentified material. Previous studies using $V_{tot,Chem}$ as the total volume concentration of aerosol particles have avoided the discussion about influences of unidentified material by the ACSM or other aerosol mass spectrometer instruments. The hygroscopicity of these unidentified materials, which might be dust or other components in continental regions, were not discussed before. Dust is nearly hydrophilic, with mineral dust showing κ in range of 0.01 to 0.08 (Koehler et al., 2009). In this paper, we arbitrarily specified κ_X to be 0.05.

https://doi.org/10.5194/acp-2019-633
Preprint. Discussion started: 30 September 2019

Atmospheric Chemistry and Physics Discussions

3.3 Can $\kappa_{f(\mathrm{RH})}$ represent κ_{chem}?

According to Eq.5, the measured bulk κ_{chem} values are needed to derive κ_{Org}. Bulk aerosol chemical compositions and aerosol hygroscopicity $\kappa_{f(\mathrm{RH})}$ measurements are available, one would naturally jump to the conclusion of treating $\kappa_{f(\mathrm{RH})}$ as κ_{chem} to derive κ_{Org} (both are from bulk aerosol measurements). However, the relationship between κ_{chem}, $\kappa_{f(\mathrm{RH})}$ and the size-resolved κ distribution needs to be clarified in order to answer the question whether $\kappa_{f(\mathrm{RH})}$ can accurately represent κ_{chem}.

Using V_i to represent volume concentrations of chemical species *i* and $V_i(D_p)$ to represent volume concentrations of species *i* with particle diameter of D_p, κ_{chem} can be derived as follows based on Eq.2,:

$$\kappa_{chem} = \sum_i \kappa_i \cdot \varepsilon_i = \sum_i \frac{V_i}{V_{tot}} \cdot \kappa_i = \sum_i \frac{1}{V_{tot}} \cdot \int \frac{d\,V_i(D_p)}{dlogD_p} \cdot dlogD_p \cdot \kappa_i. \quad (6)$$

By swapping the order of summation and integration, Eq.6 can be written as:

$$\kappa_{chem} = \int \frac{1}{V_{tot}} \cdot \sum_i \frac{d\,V_i(D_p)}{dlogD_p} \cdot dlogD_p \cdot \kappa_i. \quad (7)$$

Considering that $\kappa_{D_p} = \sum_i \frac{dV_i(D_p)}{dV(D_p)} \cdot \kappa_i$, Eq.7 can be rewritten as:

$$\kappa_{chem} = \frac{1}{V_{tot}} \int \kappa_{D_p} \cdot dV(D_p) \quad (8)$$

Result of Eq.8 indicates that κ_{chem} calculated using Eq.3 represents the overall hygroscopicity of aerosol particles with volume contribution as the weighting function of κ_{D_p}.

As for $\kappa_{f(\mathrm{RH})}$, a detailed analysis is performed here to facilitate its physical understanding. The differential form of σ_{sp} of aerosol particles in dry state can be expressed as follows:

$$\sigma_{sp} = \int \frac{d\sigma_{sp}}{dlogD_p} dlogD_p \quad (9)$$

Based on the definition of $f(\mathrm{RH})$, σ_{sp} of aerosol particles under different RH conditions can be written as:

$$\sigma_{sp}(RH) = \int \frac{d\sigma_{sp}}{dlogD_p} \cdot f_{D_p}(RH) \cdot dlogD_p \quad (10)$$

Therefore, the differential form of observed overall $f(\mathrm{RH})$ can be formulated as:

https://doi.org/10.5194/acp-2019-633
Preprint. Discussion started: 30 September 2019

Atmospheric Chemistry and Physics Discussions

336 $$f(\mathrm{RH}) = \int \frac{1}{\sigma_{sp}} \cdot \frac{d\sigma_{sp}}{dlogD_p} \cdot f_{D_p}(RH) \cdot dlogD_p \quad (11)$$

337 Based on this formula, the sensitivity of $f(\mathrm{RH})$ on the hygroscopicity of aerosol particles with
338 diameter D_p (κ_{D_p}) can be derived as:

339 $$\frac{1}{dlogD_p} \cdot \frac{\partial f(\mathrm{RH})}{\partial \kappa_{D_p}} = \frac{1}{\sigma_{sp}} \cdot \frac{d\sigma_{sp}}{dlogD_p} \cdot \frac{\partial f_{D_p}(RH)}{\partial \kappa_{D_p}} . \quad (12)$$

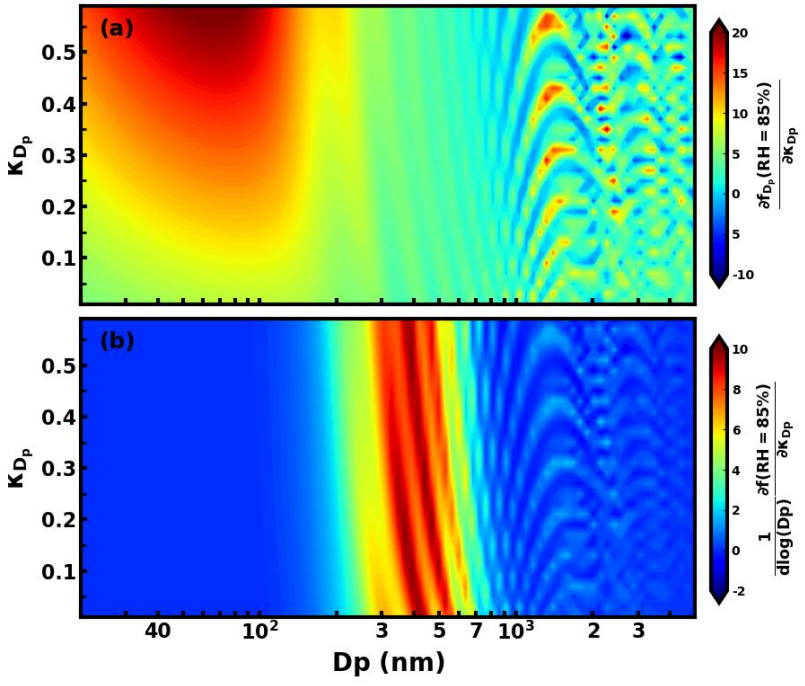

Figure 2. **(a)** simulated $\frac{\partial f_{D_p}(RH)}{\partial \kappa_{D_p}}$; **(b)** simulated $\frac{1}{dlogD_p} \cdot \frac{\partial f(\mathrm{RH})}{\partial \kappa_{D_p}}$

340 The sensitivity of $f(\mathrm{RH})$ to κ_{D_p} are determined together by the two terms in Eq. 12: (1) $\frac{1}{\sigma_{sp}} \cdot \frac{d\sigma_{sp}}{dlogD_p}$,
341 which represents the contribution of σ_{sp} of aerosol particles in dry state with diameter D_p to total
342 σ_{sp}, and (2) $\frac{\partial f_{D_p}(RH)}{\partial \kappa_{D_p}}$, which represents the sensitivity of $f_{D_p}(RH)$ to κ_{D_p}. Based on the Mie theory
343 and the κ-Köhler theory, we simulated the second term under 85% RH condition for varying D_p and
344 κ_{D_p} values (Fig.2a). In the diameter range below 200 nm, $\frac{\partial f_{D_p}(RH)}{\partial \kappa_{D_p}}$ is very high, displaying a
345 maximum near 60 nm. In this diameter range, larger κ_{D_p} generally corresponded to higher $\frac{\partial f_{D_p}(RH)}{\partial \kappa_{D_p}}$.

https://doi.org/10.5194/acp-2019-633
Preprint. Discussion started: 30 September 2019

Atmospheric Chemistry and Physics Discussions

For $200\ \text{nm} < D_p < 800\ \text{nm}$, higher and lower $\frac{\partial f_{D_p}(RH)}{\partial \kappa_{D_p}}$ appear alternatively, with all values staying positive. For $D_p > 800\ nm$, maxima and minima regions appear alternatively, and $f_{D_p}(RH)$ might decrease with increasing κ_{D_p}. This is because, at this diameter range, the aerosol scattering efficiency has a non-monotonic response to the particle diameter increase (see Fig.2a of (Kuang et al., 2018)).

The first term of Eq.9, representing size-resolved σ_{sp} contributions of particles with diameter in dry state, mainly depends on the PNSD. The average PNSD of PM_{10} was applied in the simulation the first term using Mie theory (Fig.S3). Combining results of the first term and second term, the sensitivity of $f(\text{RH})$ to κ_{D_p} was obtained and depicted in Fig.2b. Results reveal that $f(\text{RH})$ is quite sensitive to the κ_{D_p} of particles within 200 to 800 nm diameter range, but almost insensitive to κ_{D_p} of particles with diameters below 200 nm and above 800 nm (corresponding aerodynamic diameter of about 1 μm). For particles smaller than 200 nm, the first term was quite small especially for particles smaller than 100 nm (Fig.S3), while for particles larger than 800 nm, in addition to a small first term, the second term fluctuated between negative and positive values, which is why $f(\text{RH})$ was not sensitive to the overall hygroscopicity of these larger aerosol particles. These results suggest that although $\kappa_{f(\text{RH})}$ was derived from $f(\text{RH})$ measurements of PM_{10}, it mainly represents the overall hygroscopicity of aerosol particles with dry diameters between 200 and 800 nm for continental aerosols. This result indicates that $\kappa_{f(\text{RH})}$ derived from $f(\text{RH})$ measurements of PM_{10} and PM_1 should differ little from each other for measurements conducted in continental regions.

However, the quantitative relationship between $\kappa_{f(\text{RH})}$ and size-resolved κ_{D_p} is still not clear. Based on Eq.11, $f_{D_p}(RH)$ can be expressed as:

$$f_{D_p}(RH) = \frac{d\sigma_{sp}(RH)}{d\sigma_{sp}} = \frac{\frac{1}{4}\pi\cdot(D_p\cdot g)^2\cdot Q_{sca}(D_p,g)\cdot dN}{d\sigma_{sp}}, \quad (13)$$

where g is the growth factor of aerosol particles which is a function of κ_{D_p} and RH (Brock et al., 2016), i.e. $g = (1 + \kappa_{D_p}\cdot\frac{RH}{100-RH})^{1/3}$, dN is differential form of aerosol number concentration, and Q_{sca} is the scattering efficiency as a function of D_p and g. The results of Kuang et al. (2018) indicate that, under dry state, Q_{sca} can expressed as $Q_{sca} = k\cdot D_p$ with k varying as a function of D_p. Here,

https://doi.org/10.5194/acp-2019-633
Preprint. Discussion started: 30 September 2019

Atmospheric Chemistry and Physics Discussions

we follow this idea and express the Q_{sca} under humidified condition as $Q_{sca}(D_p, g) = \mathrm{C} \cdot D_p \cdot g$, where C is a function of D_p, κ_{D_p} and RH. Replacing g and Q_{sca} in Eq.13, we yield:

$$f_{D_p}(RH) = \frac{\frac{1}{4}\pi \cdot {D_p}^3 \cdot C(\mathrm{Dp},\kappa_{D_p},\mathrm{RH}) \cdot (1+\kappa_{D_p} \cdot \frac{RH}{100-RH}) \cdot dN}{d\sigma_{sp}}, \quad (14)$$

which we can substitute into Eq.8, to obtain a new expression for $f(\mathrm{RH})$:

$$f(\mathrm{RH}) = \int \frac{\frac{1}{4}\pi \cdot {D_p}^3 \cdot C(\mathrm{Dp},\kappa_{D_p},\mathrm{RH}) \cdot (1+\kappa_{D_p} \cdot \frac{RH}{100-RH}) \cdot dN}{\sigma_{sp}} \quad (15)$$

If we define $X_c(\mathrm{Dp},\kappa_{D_p},\mathrm{RH}) = C(\mathrm{Dp},\kappa_{D_p},\mathrm{RH})/\mathrm{k}$, and considering that $d\sigma_{sp} = \frac{1}{4} \cdot \pi \cdot {D_p}^2 \cdot Q_{sca} \cdot dN = \frac{1}{4} \cdot \pi \cdot {D_p}^3 \cdot \mathrm{k} \cdot dN$, Eq.14 can be written as:

$$f(\mathrm{RH}) = \int \frac{X_c(\mathrm{Dp},\kappa_{D_p},\mathrm{RH}) \cdot (1+\kappa_{D_p} \cdot \frac{RH}{100-RH}) \cdot d\sigma_{sp}}{\sigma_{sp}} \quad (16)$$

The $\kappa_{f(\mathrm{RH})}$ is a uniform κ for aerosol particle sizes that can yield simulated $f(\mathrm{RH})$ equal to the measured one. Thus, $f(\mathrm{RH})$ can also be expressed as:

$$f(\mathrm{RH}) = \int \frac{X_c(\mathrm{Dp},\kappa_{f(\mathrm{RH})},\mathrm{RH}) \cdot (1+\kappa_{f(\mathrm{RH})} \cdot \frac{RH}{100-RH}) \cdot d\sigma_{sp}}{\sigma_{sp}} \quad (17)$$

Combining Eq.16 and Eq.17, the relationship between $\kappa_{f(\mathrm{RH})}$ and size-resolved κ_{D_p} can be derived as:

$$\kappa_{f(\mathrm{RH})} = \frac{\int X_c(\mathrm{Dp},\kappa_{D_p},\mathrm{RH}) \cdot \kappa_{D_p} \cdot d\sigma_{sp}}{\int X_c(\mathrm{Dp},\kappa_{f(\mathrm{RH})},\mathrm{RH}) \cdot d\sigma_{sp}} + \frac{\int (X_c(\mathrm{Dp},\kappa_{D_p},RH) - X_c(\mathrm{Dp},\kappa_{f(\mathrm{RH})},\mathrm{RH})) \cdot d\sigma_{sp}}{\int X_c(\mathrm{Dp},\kappa_{f(\mathrm{RH})},\mathrm{RH}) \cdot d\sigma_{sp}} \cdot \frac{100-RH}{RH}. \quad (18)$$

X_c values under 85% RH for different D_p and κ_{D_p} values are simulated and shown in Fig.3, based

https://doi.org/10.5194/acp-2019-633
Preprint. Discussion started: 30 September 2019

Atmospheric Chemistry and Physics Discussions

on which the second term of Eq.18 (which depends on the PNSD and size-resolved κ_{D_p}) could be

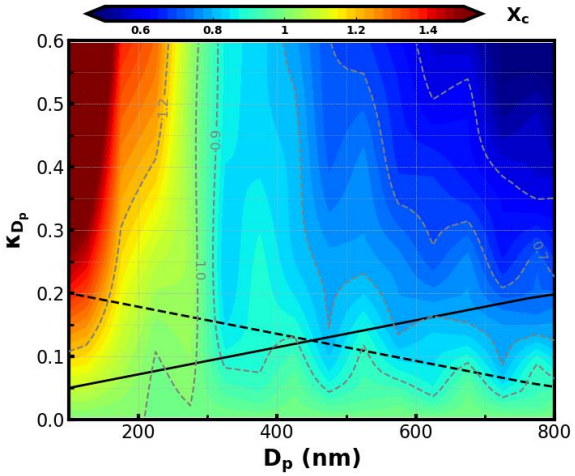

Figure 3. Simulated values of X_c under 85% RH for different D_p and κ_{D_p} values. Black solid and dashed lines are two assumed size-resolved κ_{D_p} distributions.

calculated using the average PNSD during this field campaign and two assumed extreme cases of size-resolved κ_{D_p} (solid and dashed black lines in Fig.3). For PM_1, the second term corresponding to the two size-resolved κ_{D_p} cases were -0.007 and 0.008, respectively. Corresponding values simulated for PM_{10} were -0.005 and 0.004, respectively. To further investigate the possible contribution range of the second term to $\kappa_{f(\mathrm{RH})}$, size-resolved κ_{D_p} derived by Liu et al. (2014) based on size resolved chemical composition measurements in ambient atmosphere on the NCP region (Fig.S4) were used with the average PNSD during this campaign to calculate values of the second term. Calculated values of second term ranged from -0.005 to 0.009, with its contribution to $\kappa_{f(\mathrm{RH})}$ ranging from -1.5% to 2%

https://doi.org/10.5194/acp-2019-633
Preprint. Discussion started: 30 September 2019

Atmospheric Chemistry and Physics Discussions

(0.3% on average). These results indicate that the second term was negligible in most cases, and Eq.18 could be approximated as:

$$\kappa_{f(\mathrm{RH})} \approx \frac{\int X_c(\mathrm{Dp},\kappa_{D_p},\mathrm{RH})\cdot\kappa_{D_p}\cdot d\sigma_{sp}}{\int X_c(\mathrm{Dp},\kappa_{f(\mathrm{RH})},\mathrm{RH})\cdot d\sigma_{sp}} \quad (19)$$

X_c values shown in Fig.3 indicate that for aerosol particles in the diameter range of 200 to 800 nm (which contribute most to σ_{sp} and is the part of the aerosol population $\kappa_{f(\mathrm{RH})}$ is most sensitive to) and for the observed κ_{D_p} range of continental aerosols (κ_{D_p} usually less than 0.5), X_c mainly ranged from 0.7 to 1. Considering this, we might approximately assume X_c in Eq.18 as a constant value. Then, Eq.19 can be further simplified to:

$$\kappa_{f(\mathrm{RH})} \approx \frac{1}{\sigma_{sp}} \int \kappa_{D_p} \cdot d\sigma_{sp} \quad (20)$$

This result suggests that $\kappa_{f(\mathrm{RH})}$ can be approximately understood as the overall hygroscopicity of aerosol particles with the σ_{sp} contribution as the weighting function of κ_{D_p}.

Based on results of Eq.8 and 20, both $\kappa_{f(\mathrm{RH})}$ and κ_{chem} represent the overall hygroscopicity of bulk aerosol particles, however, their weighting functions of κ_{D_p} are different. Within a certain D_p range, aerosol σ_{sp} is approximately proportional to aerosol volume (Kuang et al., 2018), resulting in little difference between $\kappa_{f(\mathrm{RH})}$ and κ_{chem}. In this study, bulk $\kappa_{f(\mathrm{RH})}$ was measured for both PM_1 and PM_{10}. How much does κ_{chem} differ from $\kappa_{f(\mathrm{RH})}$ for PM_1 and PM_{10} samples? Both PNSD and size-resolved κ_{D_p} distributions contribute to the difference between κ_{chem} and $\kappa_{f(\mathrm{RH})}$. To study

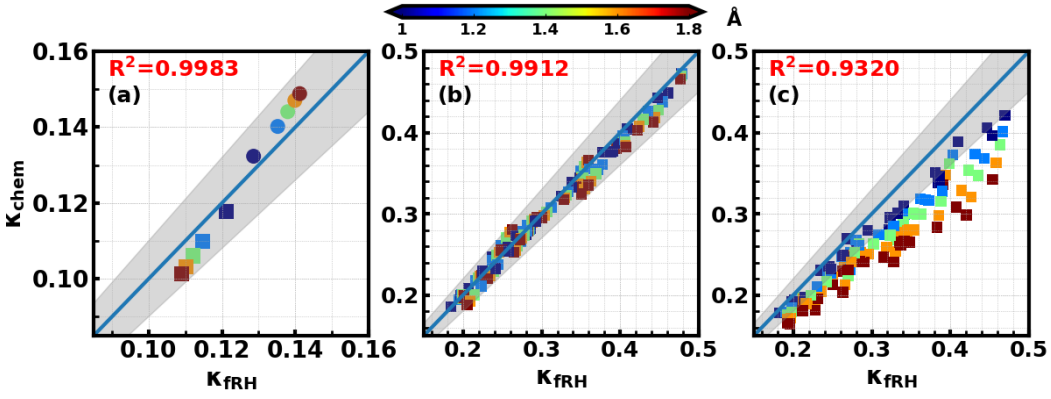

Figure 4. κ_{chem} versus $\kappa_{f(\mathrm{RH})}$, colors represent average Ångström exponent (Å) values of corresponding PNSD **(a)**corresponding to size-resolved κ_{D_p} distributions shown in Fig.4; **(b)** and **(c)** corresponding to size-resolved κ_{D_p} distributions shown in Fig.S4 for PM1 and PM10, respectively. Gray areas represent the absolute relative differences between κ_{chem} and $\kappa_{f(\mathrm{RH})}$ are less than 10%.

https://doi.org/10.5194/acp-2019-633
Preprint. Discussion started: 30 September 2019

Atmospheric Chemistry and Physics Discussions

their influences in a simple and apparent way, κ_{chem} and $\kappa_{f(\mathrm{RH})}$ were simulated based on the two extreme cases of size-resolved κ_{D_p} distributions in Fig. 3 and five average PNSDs corresponding to five ranges of aerosol Ångström exponent (0.9-1.1,1.1-1.3,1.3-1.5,1.5-1.7,1.7-1.9) during this field campaign. In the instance of PM_1, as can be seen in Fig.4a, assuming a κ_{D_p} increasing as a function of D_p resulted in $\kappa_{chem}<\kappa_{fRH}$ (square points in Fig.4a), especially for PNSDs corresponding to larger Ångström exponents. This is because the volume contributions of small particles (e.g. particles with D_p between 100 to 300 nm) to V_{tot} are larger than their light scattering coefficient contributions to σ_{sp} (as shown in Fig.S6), thus the hygroscopicity of small particles had larger impacts on κ_{chem} than κ_{fRH}. Higher Ångström exponents generally correspond to shift in PNSD towards smaller D_p, which exacerbates the contribution of small particles, further increasing the difference between κ_{chem} and κ_{fRH}. For the case with κ_{D_p} decreasing as a function of D_p (circle markers in Fig.4a) it is vice versa, resulting in $\kappa_{chem}>\kappa_{fRH}$. In general, for these two extreme cases of size-resolved κ_{D_p} distributions, the absolute value of the relative difference between κ_{chem} and $\kappa_{f(\mathrm{RH})}$ ranged from 2.8% to 7.5% with an average of 4.8%. This result indicates that for PM_1, κ_{chem} might differ little from $\kappa_{f(\mathrm{RH})}$ since κ_{D_p} usually varies less with D_p in ambient atmosphere than in the two assumed cases (Liu et al., 2014). The average size-resolved κ_{D_p} distribution from Haze in China campaign (Liu et al., 2014) indicate that κ_{D_p} varies significantly for D_p<250 nm, while it varies less within the diameter range of 250 nm to 1 μm. To further study the variation range of the relative difference between κ_{chem} and $\kappa_{f(\mathrm{RH})}$ under ambient conditions, the size-resolved κ_{D_p} distributions derived from measured size-resolved chemical compositions in the NCP region (Liu et al., 2014) (shown in Fig.S5) were used in simulations and results are shown in Fig.4b. The absolute value of the relative difference between κ_{chem} and $\kappa_{f(\mathrm{RH})}$ ranged from 0.04% to 8% with an average and standard deviation of 2.8±2%, which further confirms that for PM_1 $\kappa_{f(\mathrm{RH})}$ can accurately represent κ_{chem} in most cases.

For PM_{10}, values of κ_{chem} and $\kappa_{f(\mathrm{RH})}$ using κ_{D_p} size distributions derived from ambient measurements were simulated and displayed in Fig.4c. The simulated absolute values of the relative

https://doi.org/10.5194/acp-2019-633
Preprint. Discussion started: 30 September 2019

Atmospheric Chemistry and Physics Discussions

difference between κ_{chem} and $\kappa_{f(\mathrm{RH})}$ ranged from 0.2% to 41% with an average and standard deviation of 16±8 %, with all κ_{chem} lower than $\kappa_{f(\mathrm{RH})}$. This is because, for PM10, super-micron particles typically with low hygroscopicity (Fig.S4) contribute much more to V_{tot} than to σ_{sp} (as shown in Fig.S7). These results indicate that, for PM10, $\kappa_{f(\mathrm{RH})}$ cannot accurately represent κ_{chem}.

Above analysis results indicate that $\kappa_{f(\mathrm{RH})}$ retrieved from light scattering measurements of PM_1 represent accurately the κ_{chem} of PM_1 and can be used in Eq.5 as measured κ_{chem} for deriving κ_{Org}.

4 Results and discussions

4.1 Overview of the campaign data

The timeseries of ambient RH, chemical compositions of $PM_{2.5}$ and PM_1, σ_{sp} at 525 nm of PM_{10} and PM_1 in dry state, calculated κ_{sca} and $\kappa_{f(\mathrm{RH})}$ values of PM_{10} and PM_1 are shown in Fig.5. Overall, the mass concentrations of NR-$PM_{2.5}$ and NR-PM_1 ranged from 1 to 221 $\mu g/cm^3$ and from 1.8 to 326 $\mu g/cm^3$, with average concentrations of 63 and 93 $\mu g/cm^3$, respectively. Measured σ_{sp} at 525 nm of PM_{10} and PM_1 ranged from 11 to 1875 Mm^{-1} and from 18 to 2732 Mm^{-1}, with average values of 550 and 814 Mm^{-1}, respectively. These results demonstrate that this campaign was carried out at a site that is overall very polluted, quite clean conditions as well as extremely polluted conditions were experienced during the measurement period. The mass contributions of ammonium, nitrate, sulfate and organics to NR-$PM_{2.5}$ and NR-PM_1 are listed in Table 2, which show that on average organics contributed most to the mass concentration of NR-PM_1 and NR-$PM_{2.5}$. During the first period,

https://doi.org/10.5194/acp-2019-633
Preprint. Discussion started: 30 September 2019

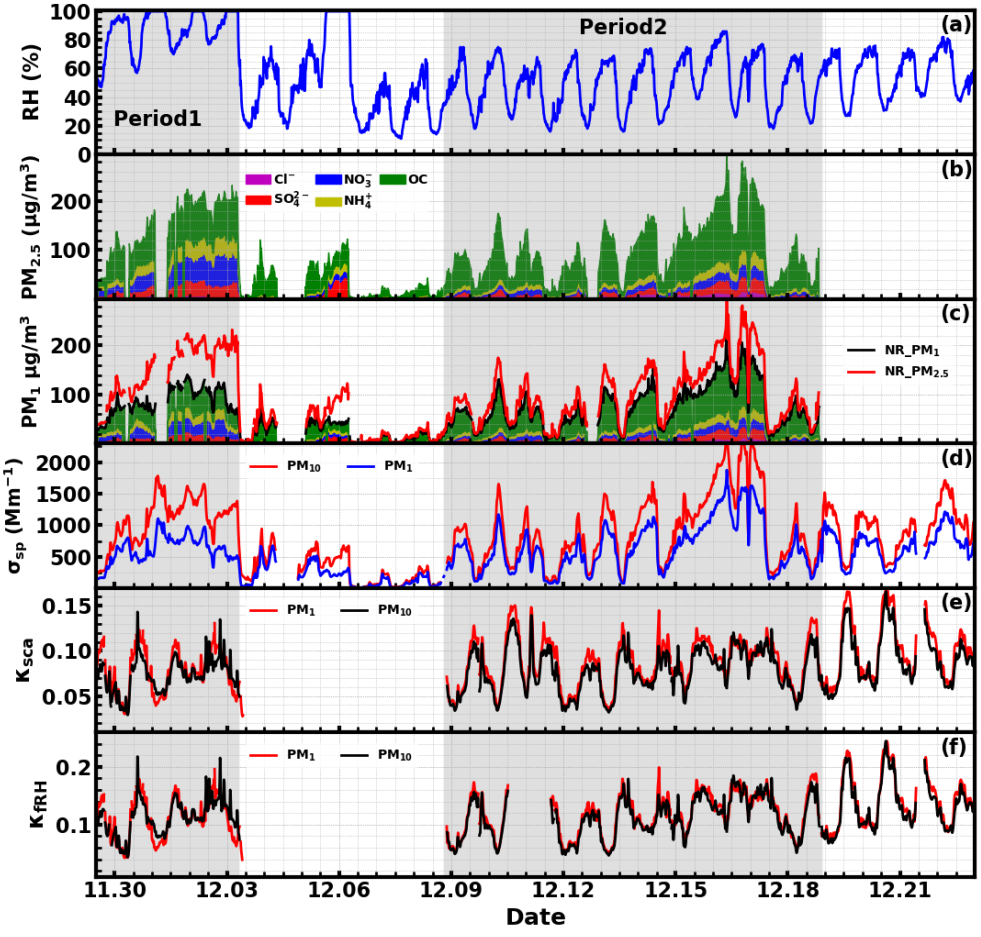

Figure 5. timeseries of ambient RH (a), chemical compositions of $PM_{2.5}$ (b) and PM_1 (c), σ_{sp} at 525 nm of PM_{10} and PM_1 (d), calculated κ_{sca} (e) and $\kappa_{f(RH)}$ (f) values of PM_{10} and PM_1.

nitrate contributed most to inorganics, while inorganics contribute most to mass concentrations of NR-$PM_{2.5}$ and NR-PM_1. During the second period, the ambient RH is relatively lower than that of the first period, ranging from 16% to 86% with an average of 49%. During this period, organics contributed most to mass concentrations of NR-$PM_{2.5}$ and NR-PM_1, with the NR mass concentrations of PM2.5 and σ_{sp} at 525 nm of PM_{10} being only 33% and 40% higher than those of PM_1.

The time series of calculated κ_{sca} and $\kappa_{f(RH)}$ are shown in Fig.5e-f. κ_{sca} of PM_1 and PM_{10} ranged in between 0.01 to 0.2 and 0.02 to 0.17, with corresponding averages of 0.09 and 0.08. From near 12:00 on the 10th Dec to about 12:00 on the 11th Dec, the $\kappa_{f(RH)}$ was not available due to the absence of PNSD measurements during that period. $\kappa_{f(RH)}$ of PM_1 and PM_{10} respectively ranged

https://doi.org/10.5194/acp-2019-633
Preprint. Discussion started: 30 September 2019

Atmospheric Chemistry and Physics Discussions

from 0.02 to 0.27 and from 0.03 to 0.26, with corresponding averages of 0.12 and 0.12. These results indicate that the hygroscopicity during this campaign was generally low, which could be associated with the high mass contributions of organics. The range as well as the average level of $\kappa_{f(\mathrm{RH})}$ is quite consistent with the results obtained from another field campaign conducted at the same site in winter 2016, suggesting low aerosol hygroscopicity conditions in winter to be prevalent at this site. Additionally, it can be noted that except for fog events, κ_{sca} and $\kappa_{f(\mathrm{RH})}$ values of PM_1 are generally higher than those of PM_{10}, however, with relative small differences (10% and 3.5% for κ_{sca} and $\kappa_{f(\mathrm{RH})}$, respectively). Although particles with diameters above 800 nm impact almost negligibly on retrieved $\kappa_{f(\mathrm{RH})}$ (refer to discussions in Sect3.3), it can still cause a small difference between $\kappa_{f(\mathrm{RH})}$ of PM10 and PM1. Results of previous studies indicate that the overall hygroscopicity of aerosol particles larger than 800 nm are usually low and are typically lower than the overall hygroscopicity of accumulation mode particles (Liu et al., 2014), which may explain why $\kappa_{f(\mathrm{RH})}$values of PM_1 are generally higher than those of PM_{10} during non-fog periods.

Table 2. Average (range) mass contribution of ammonium, nitrate, sulfate and organics to NR-PM2.5 and NR-PM1 during different periods.

Species	Ammonium		nitrate		sulfate		Organics	
	PM_1	$PM_{2.5}$	PM_1	$PM_{2.5}$	PM_1	$PM_{2.5}$	PM_1	$PM_{2.5}$
Entire	12%	12%	13%	14%	10%	11%	59%	59%
period	0.2-24%	0.1-24%	2-31%	1-32%	0.3-49%	0.2-50%%	12-99%	4-91%
Period 1	15%	16%	22%	24%	13%	14%	47%	42%
Fog	10-17%	12-18%	11-28%	16-30%	9-15%	12-16%	30-65%	37-55%
Period 1	17%	16%	23%	23%	12%	12%	43%	44%
non-fog	10-22%	7-21%	6-31%	5-32%	8-23%	7-17%	32-75%	31-69%
Period 2	12%	10%	11%	10%	8%	7%	64%	67%
	0.2-20%	0.1-19%	5-30%	4-29%	0.3-16%	0.2-16%	40-82%	40-85%

During fog periods, a large part of submicron particles in dry state will activate into fog droplets, which are super micron particles in ambient state (see PNSD example in Fig.S4a), exerting substantial impacts on $f(\mathrm{RH})$ measurements of PM_{10} which are not detectable in the PM_1 measurements. Since for a certain particle diameter and fog supersaturation, particles with higher hygroscopicity are more

https://doi.org/10.5194/acp-2019-633
Preprint. Discussion started: 30 September 2019

Atmospheric Chemistry and Physics Discussions

readily activated, the observed PM_{10} $\kappa_{f(RH)}$ increased during fog events and often exceeded those of PM_1 in contrast to non-fog periods (Fig.5f).

4.2 κ_{Org} derivations and its relationship with organic aerosol oxidation state

The discussion results in Sect.3.3 demonstrate that $\kappa_{f(RH)}$ of PM_1 accurately represents κ_{chem} in most cases, thus a closure study between calculated κ_{chem} of PM_1 based on measured chemical compositions and measured κ_{chem} (represented by PM_1 $\kappa_{f(RH)}$) can be conducted using Eq.3 if κ_{Org} were a known parameter. A κ_{Org} of 0.06 was used in this closure test, which was the calculated by Wu et al. (2016) based on aerosol chemical composition and aerosol hygroscopicity measurements. The comparison between measured and calculated κ_{chem} as shown in Fig.6a has not achieved very

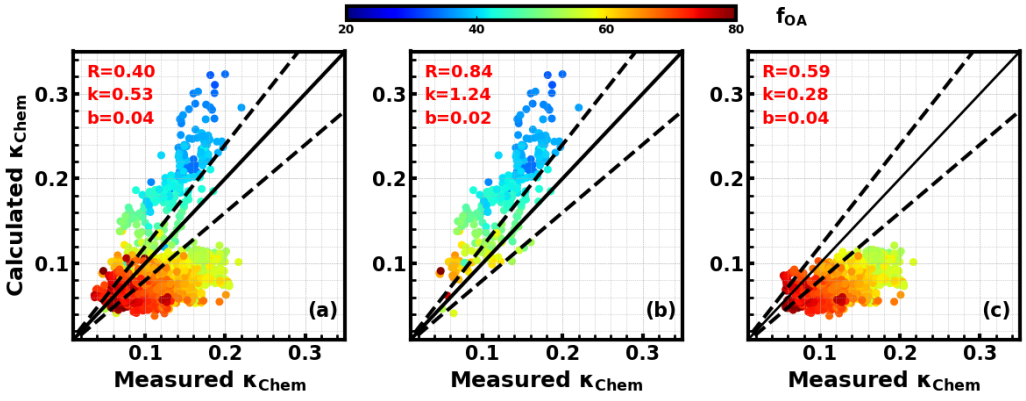

Figure 6. Comparison between measured and calculated κ_{chem} by assuming a κ_{Org} of 0.06. **(a)** The whole period; **(b)** Only Period 1; **(c)** Only Period 2. Colors represents the mass fractions of organic aerosol in NR-PM1 (f_{OA}), and the color bar is shown on the top.

good agreement. On one hand, calculated κ_{chem} overestimated the measured one when mass fractions of organic aerosol (f_{OA}) was lower than 45%, while on the other hand calculated κ_{chem} underestimated the measured one in most cases when f_{OA} was higher than 45%. As introduced in Sect.4.1, these two situations roughly correspond to situations of Period 1 and 2, respectively. Separating the data points shown in Fig.6a into Periods 1 (Fig.7b) and 2 (Fig.7c), it can be seen that all low f_{OA} data points are found in Period 1, with most of the data points showing f_{OA} less than 50%. Although the calculated κ_{chem} during this period was on average 25% higher than the measured κ_{chem}, they were highly correlated (R=0.84). A similar case was also found in Wu et al. (2013), and they conclude that the loss of ammonium nitrate (semi volatile particles) in the HTDMA might be the

https://doi.org/10.5194/acp-2019-633
Preprint. Discussion started: 30 September 2019

Atmospheric Chemistry and Physics Discussions

503 reason. The relationship between nitrate concentration and the difference between calculated and
504 measured κ_{chem} was investigated, which confirmed that the discrepancy was highly correlated to
505 mass fractions of nitrate in NR-PM1(Fig.S7), suggesting that the overestimation of calculated κ_{chem}
506 might be associated with the volatile loss of ammonium nitrate. Since the tube length (from the splitter
507 to inlet of instrument) of wet nephelometer was about 1 m longer than that of the ACSM, there probably
508 was more loss in ammonium nitrate in the wet nephelometer.

509 During Period 2, the average mass fraction of nitrate was low (11%), which is why the loss of
510 ammonium nitrate had little influence on κ_{chem} estimations (Fig.S7). However, during Period 2,
511 when organic aerosol was the dominating, the calculated κ_{chem} underestimated measured κ_{chem} in
512 most cases (Fig.6c). Previous studies have shown larger κ_{Org} for OA with higher oxidation level
513 (Chang et al., 2010;Duplissy et al., 2011;Wu et al., 2013), which might have contributed to the
514 underestimation in κ_{chem}. This gave us the hint that Period 2 might provide us with a good opportunity
515 to study κ_{Org}. Following the method in Sect. 3.2, κ_{Org} was derived using Eq.5, resulting in a κ_{Org}

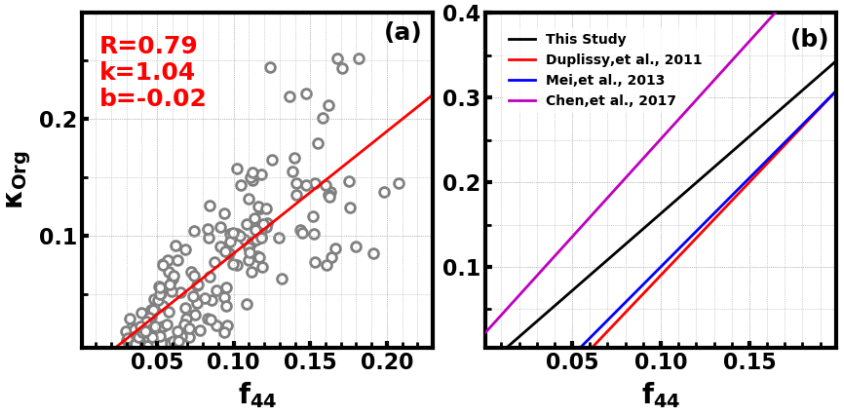

Figure 7. **(a)** the relationship between derived κ_{Org} and f_{44}; **(b)** Comparison with earlier studies.

516 ranging from 0.0 to 0.25, with an average of 0.08±0.06. This indicates that using a constant κ_{Org}
517 value in the calculation of κ_{chem} would result in large bias. To further investigate the impact of OA
518 oxidation level on κ_{Org}, we compared the derived κ_{Org} against f_{44}, which is often used to represent
519 the oxidation level of OA. Results show a clear positive correlation (R=0.79) and a statistical
520 relationship of $\kappa_{Org} = 1.04 \cdot f_{44}$ - 0.02 (Fig.7a), indicating that the degree of oxidation level is a
521 crucial parameter determining the OA hygroscopicity. The derived empirical relationship between

https://doi.org/10.5194/acp-2019-633
Preprint. Discussion started: 30 September 2019

Atmospheric Chemistry and Physics Discussions

522 κ_{Org} and f_{44} was compared to results in earlier studies (Fig.7b). As mentioned in Sect.2.3, f_{44} from
523 CV-ToF-ACSM measurements is much higher than those previously reported from AMS, but they are
524 well correlated and the ratio between f_{44} of CV-ToF-ACSM and previous AMS instruments for
525 ambient aerosol ranges from 1.5 to 2 with an average of 1.75. Therefore, to be consistent with the f_{44}
526 in previous studies, the empirical relationship in Fig.7b is changed to $\kappa_{Org} = 1.79 \cdot f_{44}$ - 0.03. The
527 κ_{Org} values are lower than that from the scheme of Chen et al. (2017), but higher than those in
528 Duplissy et al. (2011) and Mei et al. (2013a). In general, results of all published studies demonstrate
529 that hygroscopicity of organic aerosol generally increase as the oxidation level of organic aerosol
530 increases, however, the empirical mathematical relationship differs much among different studies
531 (Hong et al., 2018). These results highlight that more studies are required to study the influence of OA
532 oxidation level on κ_{Org} to approach a more universal parameterization scheme that can be used in
533 chemical, meteorological and climate models.

534 **4.3 Distinct diurnal variations of κ_{Org} and its relationship with OOA**

535 The discussions in Sect. 4.2 already proved that κ_{Org} was highly variable, which is why we need
536 to know its variational characteristics and influencing factors. The time series of derived κ_{Org} is
537 depicted in Fig.8a, showing large κ_{Org} fluctuations within a day. The average diurnal profile of κ_{Org}
538 (Fig.8b) displays a distinct diurnal variation, with κ_{Org} reaching its minimum (0.02) in the morning
539 (near 07:30 LT) and increasing quickly to a maximum (0.19) near 14:30 LT. During daytime, the water
540 uptake abilities of organic aerosol particles changed from near hydrophobic to moderately hygroscopic
541 within 7 hours. Previous results from observations in Japan also revealed significant κ_{Org} diurnal
542 variations, however, with daily minima in the afternoon hours due to the increase of less oxygenated
543 OA mass fractions (Deng et al. (2018) and Deng et al. (2019)). Such large variability and significant
544 diurnal variations of κ_{Org} were observed for the first time on the NCP.

https://doi.org/10.5194/acp-2019-633
Preprint. Discussion started: 30 September 2019

Atmospheric Chemistry and Physics Discussions

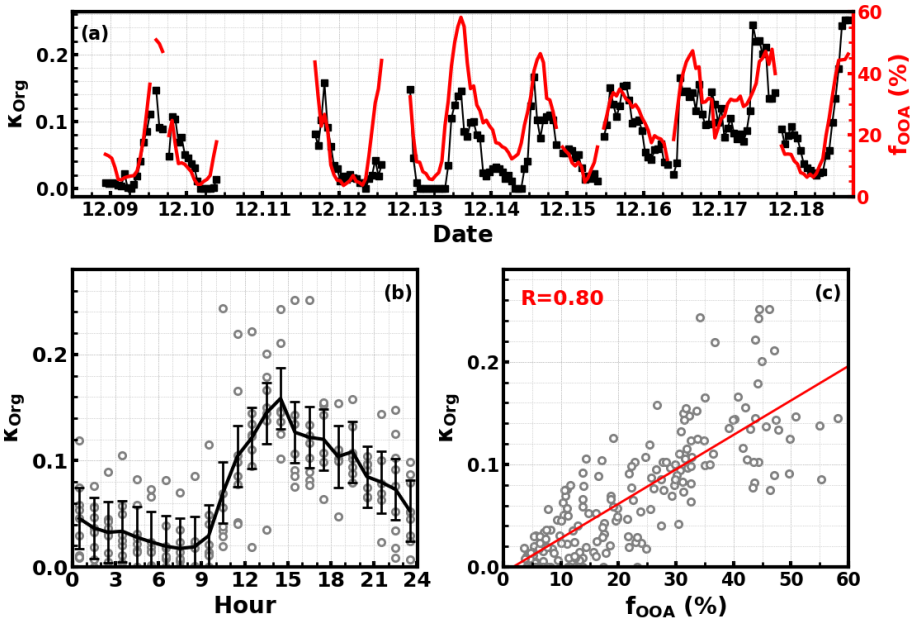

Figure 8. **(a)** Time series of derived κ_{Org} and OOA mass fraction in NR-PM1 (f_{OOA}) in the right y-axis; **(b)** Average diurnal profile of κ_{Org}; **(c)** Scatter points of κ_{Org} versus f_{OOA} (%), and red line is the fitting line with linear regression.

Results introduced in Sect.4.2 demonstrated that κ_{Org} was highly correlated to the OA oxidation level, which suggests that κ_{Org} might be associated with the oxygenated part of organic aerosol. In this study, the mass concentrations of OOA were derived using PMF analysis, and its mass fraction in the total organic aerosol mass (f_{OOA}) was calculated (Fig.8a). f_{OOA} displays diurnal variations similar to κ_{Org} and the statistical relationship between κ_{Org} and f_{OOA} (Fig.8c) shows a strong correlation (R=0.8), which both hint that OOA might be a determining factor for κ_{Org}.

The correlation coefficient between the average diurnal profiles of κ_{Org} and f_{OOA} was 0.95, which suggests that the variations in f_{OOA} was driving the significant diurnal variations of κ_{Org}. The average diurnal variations of mass concentrations of identified OOA, HOA, COA, CCOA, BBOA, and their mass fractions in total organic mass are shown in Fig.9a and Fig.9b, respectively. The mass concentrations of HOA, CCOA and BBOA decreased sharply from the morning time to about 15:00 LT due to boundary layer evolution processes. The mass concentrations of COA increased a little in the morning and then decreased quickly after 09:30 LT. This transitory increase of COA in the morning might be associated with the cooking for breakfast. However, the OOA mass increased sharply from

https://doi.org/10.5194/acp-2019-633
Preprint. Discussion started: 30 September 2019

Atmospheric Chemistry and Physics Discussions

about 07:30 to 10:30 LT even under the quick boundary layer development during this time range, remaining almost constant thereafter. The rapid decrease of primary organic aerosol components and rise in OOA concentration resulted in dramatic increase of f_{OOA} from 9:00 to 13:30 LT in the

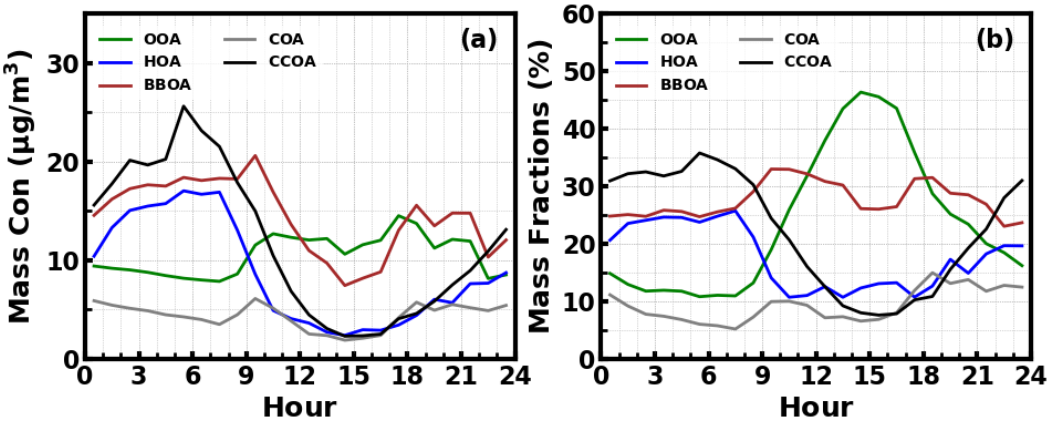

Figure 9. (a) Average diurnal profiles of mass concentrations of OOA, HOA, COA, CCOA, BBOA; (b) Average diurnal variations of mass fractions of OOA, HOA, COA, CCOA, BBOA.

afternoon, this period also corresponds to the fastest increase period of κ_{Org}. After 14:30 LT, the OOA mass concentration varied little, however, mass concentrations of primary organic aerosol components increased quickly, resulting in the decrease of f_{OOA} and κ_{Org}.

5 Conclusions

A field campaign was conducted in winter 2018 on the North China Plain, using a humidified nephelometer system and a ACSM to measure the bulk aerosol hygroscopicity of PM_{10} and PM_1 and bulk aerosol chemical compositions of $PM_{2.5}$ and PM_1.

During this field campaign, the air was highly polluted with high aerosol loadings. Measured σ_{sp} at 525 nm of PM_{10} and PM_1 in dry state ranged from 11 to 1875 Mm^{-1} and from 18 to 2732 Mm^{-1} with average values of 550 and 814 Mm^{-1}, respectively. Retrieved $\kappa_{f(\mathrm{RH})}$ of PM_{10} and PM_1 ranged between 0.02 to 0.27 and 0.03 to 0.26, with averages of 0.12 and 0.12, respectively. The $\kappa_{f(\mathrm{RH})}$ (derived from aerosol light scattering enhancement $f(\mathrm{RH})$) difference between PM_{10} and PM_1 was found to be relatively small (3.5% in average), which was consistent with the physical and mathematical interpretation of $\kappa_{f(\mathrm{RH})}$.

A method of calculating κ_{Org} (organic aerosol hygroscopicity) base on $f(\mathrm{RH})$ and bulk aerosol

https://doi.org/10.5194/acp-2019-633
Preprint. Discussion started: 30 September 2019

Atmospheric Chemistry and Physics Discussions

chemical composition measurements is proposed. The key part of this method is that the size cut of bulk aerosol chemical composition measurements should be PM_1 no matter the bulk $\kappa_{f(RH)}$ is retrieved from light scattering enhancement measurements of PM_1 or PM_{10}. The derived κ_{Org} ranged from 0.0 to 0.25 with an average of 0.08, which highlights that κ_{Org} displayed a large variability on the NCP and that large uncertainties would rise if a constant κ_{Org} were used to estimate the climatic and environmental effects of organic aerosols. The variation of κ_{Org} was significantly positively correlated to the oxidation degree of organic aerosols. In addition, a distinct diurnal variation of κ_{Org} was found, with a minimum in the morning (0.02) and maximum in the afternoon(0.16), indicating that the organic aerosol changed from near hydrophobic to near moderately hygroscopic during daytime within only 7 hours, which was observed for the first time in the NCP region. The distinct diurnal variations of κ_{Org} were associated with the significant diurnal variations of mass fractions of oxygenated organic aerosol in total organic aerosol mass. The rapid formation of oxygenated organic aerosol together with the dilution of primary organic aerosol during the development of the boundary layer resulted in the quick increase of mass fractions of oxygenated organic aerosol and κ_{Org}.

The large variability and distinct diurnal variations in κ_{Org} found in this study reveal the urgent need for more studies on the spatial and temporal variations of κ_{Org} in the NCP region to better characterize κ_{Org}. The significant influences of organic aerosol aging processes on organic aerosol hygroscopicity should be considered in studying roles of organic aerosol in cloud formation, atmospheric radiative effects and atmospheric chemistry.

Data availability. The data used in this study are available from the corresponding author upon request (kuangye@jnu.edu.cn) and (sunyele@mail.iap.ac.cn).

Competing interests. The authors declare that they have no conflict of interest.

Author Contributions. YK conceived and organized this paper. YC, HS, NM, YK and JT planned this campaign. YK, YS and NM designed the experiments. YK and YH conducted the ACSM and aerosol light scattering enhancement factor measurements. YZ and SZ conducted the particle number size distribution measurements. JS and WY conducted the black carbon measurements. YH performed the ACSM PMF analysis. WX, YH, YS, CZ, PZ and YC helped the data analysis, and WX helped

https://doi.org/10.5194/acp-2019-633
Preprint. Discussion started: 30 September 2019

Atmospheric Chemistry and Physics Discussions

much in the language editing. YK, YH and YS prepared the manuscript with contributions from all co-authors.

Acknowledgments

This work is supported by National Key Research and Development Program of China (Grant 2017YFC0210104)，National Natural Science Foundation of China (91644218), the National research program for key issues in air pollution control (DQGG0103) and the Guangdong Innovative and Entrepreneurial Research Team Program (Research team on atmospheric environmental roles and effects of carbonaceous species: 2016ZT06N263). We also thanks scientists and technicians from Max Planck Institute for Chemistry, Mainz for supporting this field campaign.

References

Bergin, M. H., Cass, G. R., Xu, J., Fang, C., Zeng, L. M., Yu, T., Salmon, L. G., Kiang, C. S., Tang, X. Y., Zhang, Y. H., and Chameides, W. L.: Aerosol radiative, physical, and chemical properties in Beijing during June 1999, J. Geophys. Res.-Atmos., 106, 17969-17980, 10.1029/2001jd900073, 2001.

Bian, Y. X., Zhao, C. S., Ma, N., Chen, J., and Xu, W. Y.: A study of aerosol liquid water content based on hygroscopicity measurements at high relative humidity in the North China Plain, Atmos. Chem. Phys., 14, 6417-6426, 10.5194/acp-14-6417-2014, 2014.

Bougiatioti, A., Bezantakos, S., Stavroulas, I., Kalivitis, N., Kokkalis, P., Biskos, G., Mihalopoulos, N., Papayannis, A., and Nenes, A.: Biomass-burning impact on CCN number, hygroscopicity and cloud formation during summertime in the eastern Mediterranean, Atmos. Chem. Phys., 16, 7389-7409, 10.5194/acp-16-7389-2016, 2016.

Brock, C. A., Wagner, N. L., Anderson, B. E., Attwood, A. R., Beyersdorf, A., Campuzano-Jost, P., Carlton, A. G., Day, D. A., Diskin, G. S., Gordon, T. D., Jimenez, J. L., Lack, D. A., Liao, J., Markovic, M. Z., Middlebrook, A. M., Ng, N. L., Perring, A. E., Richardson, M. S., Schwarz, J. P., Washenfelder, R. A., Welti, A., Xu, L., Ziemba, L. D., and Murphy, D. M.: Aerosol optical properties in the southeastern United States in summer – Part 1: Hygroscopic growth, Atmospheric Chemistry and Physics, 16, 4987-5007, 10.5194/acp-16-4987-2016, 2016.

Cerully, K. M., Bougiatioti, A., Hite Jr, J. R., Guo, H., Xu, L., Ng, N. L., Weber, R., and Nenes, A.: On the link between hygroscopicity, volatility, and oxidation state of ambient and water-soluble aerosols in the southeastern United States, Atmos. Chem. Phys., 15, 8679-8694, 10.5194/acp-15-8679-2015, 2015.

Chang, R. Y. W., Slowik, J. G., Shantz, N. C., Vlasenko, A., Liggio, J., Sjostedt, S. J., Leaitch, W. R., and Abbatt, J. P. D.: The hygroscopicity parameter (κ) of ambient organic aerosol at a field site subject to biogenic and anthropogenic influences: relationship to degree of aerosol oxidation, Atmos. Chem. Phys., 10, 5047-5064, 10.5194/acp-10-5047-2010, 2010.

https://doi.org/10.5194/acp-2019-633
Preprint. Discussion started: 30 September 2019

Atmospheric Chemistry and Physics Discussions

643 Chen, J., Zhao, C. S., Ma, N., and Yan, P.: Aerosol hygroscopicity parameter derived from the light scattering enhancement
644 factor measurements in the North China Plain, Atmos. Chem. Phys. Discuss., 14, 3459-3497, 10.5194/acpd-14-3459-2014,
645 2014.
646 Chen, J., Budisulistiorini, S. H., Itoh, M., Lee, W. C., Miyakawa, T., Komazaki, Y., Yang, L. D. Q., and Kuwata, M.: Water uptake
647 by fresh Indonesian peat burning particles is limited by water-soluble organic matter, Atmos. Chem. Phys., 17, 11591-
648 11604, 10.5194/acp-17-11591-2017, 2017.
649 Cheng, Y. F., Wiedensohler, A., Eichler, H., Su, H., Gnauk, T., Brueggemann, E., Herrmann, H., Heintzenberg, J., Slanina, J.,
650 Tuch, T., Hu, M., and Zhang, Y. H.: Aerosol optical properties and related chemical apportionment at Xinken in Pearl River
651 Delta of China, Atmospheric Environment, 42, 6351-6372, 10.1016/j.atmosenv.2008.02.034, 2008.
652 Deng, Y., Kagami, S., Ogawa, S., Kawana, K., Nakayama, T., Kubodera, R., Adachi, K., Hussein, T., Miyazaki, Y., and Mochida,
653 M.: Hygroscopicity of Organic Aerosols and Their Contributions to CCN Concentrations Over a Midlatitude Forest in Japan,
654 Journal of Geophysical Research: Atmospheres, 123, 9703-9723, 10.1029/2017jd027292, 2018.
655 Deng, Y., Yai, H., Fujinari, H., Kawana, K., Nakayama, T., and Mochida, M.: Diurnal variation and size dependence of the
656 hygroscopicity of organic aerosol at a forest site in Wakayama, Japan: their relationship to CCN concentrations, Atmos.
657 Chem. Phys., 19, 5889-5903, 10.5194/acp-19-5889-2019, 2019.
658 Drinovec, L., Močnik, G., Zotter, P., Prévôt, A. S. H., Ruckstuhl, C., Coz, E., Rupakheti, M., Sciare, J., Müller, T., Wiedensohler,
659 A., and Hansen, A. D. A.: The "dual-spot" Aethalometer: an improved measurement of aerosol black carbon with real-
660 time loading compensation, Atmospheric Measurement Techniques, 8, 1965-1979, 10.5194/amt-8-1965-2015, 2015.
661 Duplissy, J., DeCarlo, P. F., Dommen, J., Alfarra, M. R., Metzger, A., Barmpadimos, I., Prevot, A. S. H., Weingartner, E.,
662 Tritscher, T., Gysel, M., Aiken, A. C., Jimenez, J. L., Canagaratna, M. R., Worsnop, D. R., Collins, D. R., Tomlinson, J., and
663 Baltensperger, U.: Relating hygroscopicity and composition of organic aerosol particulate matter, Atmos. Chem. Phys., 11,
664 1155-1165, 10.5194/acp-11-1155-2011, 2011.
665 Fröhlich, R., Cubison, M. J., Slowik, J. G., Bukowiecki, N., Prévôt, A. S. H., Baltensperger, U., Schneider, J., Kimmel, J. R.,
666 Gonin, M., Rohner, U., Worsnop, D. R., and Jayne, J. T.: The ToF-ACSM: a portable aerosol chemical speciation monitor
667 with TOFMS detection, Atmos. Meas. Tech., 6, 3225-3241, 10.5194/amt-6-3225-2013, 2013.
668 Frosch, M., Bilde, M., DeCarlo, P. F., Jurányi, Z., Tritscher, T., Dommen, J., Donahue, N. M., Gysel, M., Weingartner, E., and
669 Baltensperger, U.: Relating cloud condensation nuclei activity and oxidation level of α-pinene secondary organic aerosols,
670 Journal of Geophysical Research: Atmospheres, 116, 10.1029/2011jd016401, 2011.
671 Gysel, M., Crosier, J., Topping, D. O., Whitehead, J. D., Bower, K. N., Cubison, M. J., Williams, P. I., Flynn, M. J., McFiggans,
672 G. B., and Coe, H.: Closure study between chemical composition and hygroscopic growth of aerosol particles during
673 TORCH2, Atmos. Chem. Phys., 7, 6131-6144, 10.5194/acp-7-6131-2007, 2007.
674 Hong, J., Kim, J., Nieminen, T., Duplissy, J., Ehn, M., Äijälä, M., Hao, L. Q., Nie, W., Sarnela, N., Prisle, N. L., Kulmala, M.,
675 Virtanen, A., Petäjä, T., and Kerminen, V. M.: Relating the hygroscopic properties of submicron aerosol to both gas- and
676 particle-phase chemical composition in a boreal forest environment, Atmos. Chem. Phys., 15, 11999-12009, 10.5194/acp-
677 15-11999-2015, 2015.
678 Hong, J., Xu, H., Tan, H., Yin, C., Hao, L., Li, F., Cai, M., Deng, X., Wang, N., Su, H., Cheng, Y., Wang, L., Petäjä, T., and
679 Kerminen, V. M.: Mixing state and particle hygroscopicity of organic-dominated aerosols over the Pearl River Delta region
680 in China, Atmos. Chem. Phys., 18, 14079-14094, 10.5194/acp-18-14079-2018, 2018.
681 Hu, W., Campuzano-Jost, P., Day, D. A., Croteau, P., Canagaratna, M. R., Jayne, J. T., Worsnop, D. R., and Jimenez, J. L.:
682 Evaluation of the new capture vapourizer for aerosol mass spectrometers (AMS) through laboratory studies of inorganic
683 species, Atmos. Meas. Tech., 10, 2897-2921, 10.5194/amt-10-2897-2017, 2017.
684 Hu, W., Day, D. A., Campuzano-Jost, P., Nault, B. A., Park, T., Lee, T., Croteau, P., Canagaratna, M. R., Jayne, J. T., Worsnop,
685 D. R., and Jimenez, J. L.: Evaluation of the new capture vaporizer for aerosol mass spectrometers: Characterization of
686 organic aerosol mass spectra, Aerosol Science and Technology, 52, 725-739, 10.1080/02786826.2018.1454584, 2018a.

https://doi.org/10.5194/acp-2019-633
Preprint. Discussion started: 30 September 2019

Atmospheric Chemistry and Physics Discussions

687 Hu, W., Day, D. A., Campuzano-Jost, P., Nault, B. A., Park, T., Lee, T., Croteau, P., Canagaratna, M. R., Jayne, J. T., Worsnop,
688 D. R., and Jimenez, J. L.: Evaluation of the New Capture Vaporizer for Aerosol Mass Spectrometers (AMS): Elemental
689 Composition and Source Apportionment of Organic Aerosols (OA), ACS Earth and Space Chemistry, 2, 410-421,
690 10.1021/acsearthspacechem.8b00002, 2018b.
691 Jimenez, J. L., Canagaratna, M. R., Donahue, N. M., Prevot, A. S. H., Zhang, Q., Kroll, J. H., DeCarlo, P. F., Allan, J. D., Coe,
692 H., Ng, N. L., Aiken, A. C., Docherty, K. S., Ulbrich, I. M., Grieshop, A. P., Robinson, A. L., Duplissy, J., Smith, J. D., Wilson, K.
693 R., Lanz, V. A., Hueglin, C., Sun, Y. L., Tian, J., Laaksonen, A., Raatikainen, T., Rautiainen, J., Vaattovaara, P., Ehn, M., Kulmala,
694 M., Tomlinson, J. M., Collins, D. R., Cubison, M. J., Dunlea, J., Huffman, J. A., Onasch, T. B., Alfarra, M. R., Williams, P. I.,
695 Bower, K., Kondo, Y., Schneider, J., Drewnick, F., Borrmann, S., Weimer, S., Demerjian, K., Salcedo, D., Cottrell, L., Griffin,
696 R., Takami, A., Miyoshi, T., Hatakeyama, S., Shimono, A., Sun, J. Y., Zhang, Y. M., Dzepina, K., Kimmel, J. R., Sueper, D., Jayne,
697 J. T., Herndon, S. C., Trimborn, A. M., Williams, L. R., Wood, E. C., Middlebrook, A. M., Kolb, C. E., Baltensperger, U., and
698 Worsnop, D. R.: Evolution of Organic Aerosols in the Atmosphere, Science, 326, 1525-1529, 10.1126/science.1180353,
699 2009.
700 Kawana, K., Nakayama, T., and Mochida, M.: Hygroscopicity and CCN activity of atmospheric aerosol particles and their
701 relation to organics: Characteristics of urban aerosols in Nagoya, Japan, Journal of Geophysical Research: Atmospheres,
702 121, 4100-4121, 10.1002/2015JD023213, 2016.
703 Koehler, K. A., Kreidenweis, S. M., DeMott, P. J., Petters, M. D., Prenni, A. J., and Carrico, C. M.: Hygroscopicity and cloud
704 droplet activation of mineral dust aerosol, Geophysical Research Letters, 36, 10.1029/2009GL037348, 2009.
705 Kuang, Y., Zhao, C., Tao, J., Bian, Y., Ma, N., and Zhao, G.: A novel method for deriving the aerosol hygroscopicity parameter
706 based only on measurements from a humidified nephelometer system, Atmos. Chem. Phys., 17, 6651-6662, 10.5194/acp-
707 17-6651-2017, 2017.
708 Kuang, Y., Zhao, C. S., Zhao, G., Tao, J. C., Xu, W., Ma, N., and Bian, Y. X.: A novel method for calculating ambient aerosol
709 liquid water content based on measurements of a humidified nephelometer system, Atmospheric Measurement
710 Techniques, 11, 2967-2982, 10.5194/amt-11-2967-2018, 2018.
711 Lambe, A. T., Onasch, T. B., Massoli, P., Croasdale, D. R., Wright, J. P., Ahern, A. T., Williams, L. R., Worsnop, D. R., Brune,
712 W. H., and Davidovits, P.: Laboratory studies of the chemical composition and cloud condensation nuclei (CCN) activity of
713 secondary organic aerosol (SOA) and oxidized primary organic aerosol (OPOA), Atmos. Chem. Phys., 11, 8913-8928,
714 10.5194/acp-11-8913-2011, 2011.
715 Li, X., Song, S., Zhou, W., Hao, J., Worsnop, D. R., and Jiang, J.: Interactions between aerosol organic components and liquid
716 water content during haze episodes in Beijing, Atmos. Chem. Phys. Discuss., 2019, 1-19, 10.5194/acp-2019-316, 2019.
717 Liu, H. J., Zhao, C. S., Nekat, B., Ma, N., Wiedensohler, A., van Pinxteren, D., Spindler, G., Müller, K., and Herrmann, H.:
718 Aerosol hygroscopicity derived from size-segregated chemical composition and its parameterization in the North China
719 Plain, Atmos. Chem. Phys., 14, 2525-2539, 10.5194/acp-14-2525-2014, 2014.
720 Liu, X., and Wang, J.: How important is organic aerosol hygroscopicity to aerosol indirect forcing?, Environmental Research
721 Letters, 5, 044010, 10.1088/1748-9326/5/4/044010, 2010.
722 Ma, N., Zhao, C. S., Nowak, A., Müller, T., Pfeifer, S., Cheng, Y. F., Deng, Z. Z., Liu, P. F., Xu, W. Y., Ran, L., Yan, P., Göbel, T.,
723 Hallbauer, E., Mildenberger, K., Henning, S., Yu, J., Chen, L. L., Zhou, X. J., Stratmann, F., and Wiedensohler, A.: Aerosol
724 optical properties in the North China Plain during HaChi campaign: an in-situ optical closure study, Atmos. Chem. Phys.,
725 11, 5959-5973, 10.5194/acp-11-5959-2011, 2011.
726 Massoli, P., Lambe, A. T., Ahern, A. T., Williams, L. R., Ehn, M., Mikkilä, J., Canagaratna, M. R., Brune, W. H., Onasch, T. B.,
727 Jayne, J. T., Petäjä, T., Kulmala, M., Laaksonen, A., Kolb, C. E., Davidovits, P., and Worsnop, D. R.: Relationship between
728 aerosol oxidation level and hygroscopic properties of laboratory generated secondary organic aerosol (SOA) particles,
729 Geophysical Research Letters, 37, 10.1029/2010gl045258, 2010.
730 Mei, F., Hayes, P. L., Ortega, A., Taylor, J. W., Allan, J. D., Gilman, J., Kuster, W., de Gouw, J., Jimenez, J. L., and Wang, J.:

https://doi.org/10.5194/acp-2019-633
Preprint. Discussion started: 30 September 2019

Atmospheric Chemistry and Physics Discussions

731 Droplet activation properties of organic aerosols observed at an urban site during CalNex-LA, Journal of Geophysical
732 Research: Atmospheres, 118, 2903-2917, 10.1002/jgrd.50285, 2013a.
733 Mei, F., Setyan, A., Zhang, Q., and Wang, J.: CCN activity of organic aerosols observed downwind of urban emissions during
734 CARES, Atmos. Chem. Phys., 13, 12155-12169, 10.5194/acp-13-12155-2013, 2013b.
735 Paatero, P., and Tapper, U.: Positive matrix factorization: A non-negative factor model with optimal utilization of error
736 estimates of data values, Environmetrics, 5, 111-126, 10.1002/env.3170050203, 1994.
737 Petters, M. D., and Kreidenweis, S. M.: A single parameter representation of hygroscopic growth and cloud condensation
738 nucleus activity, Atmospheric Chemistry and Physics, 7, 1961-1971, 2007.
739 Quinn, P. K., Coffman, D. J., Bates, T. S., Miller, T. L., Johnson, J. E., Welton, E. J., Neusüss, C., Miller, M., and Sheridan, P. J.:
740 Aerosol optical properties during INDOEX 1999: Means, variability, and controlling factors, Journal of Geophysical
741 Research: Atmospheres, 107, INX2 19-11-INX12 19-25, 10.1029/2000jd000037, 2002.
742 Rastak, N., Pajunoja, A., Acosta Navarro, J. C., Ma, J., Song, M., Partridge, D. G., Kirkevåg, A., Leong, Y., Hu, W. W., Taylor,
743 N. F., Lambe, A., Cerully, K., Bougiatioti, A., Liu, P., Krejci, R., Petäjä, T., Percival, C., Davidovits, P., Worsnop, D. R., Ekman,
744 A. M. L., Nenes, A., Martin, S., Jimenez, J. L., Collins, D. R., Topping, D. O., Bertram, A. K., Zuend, A., Virtanen, A., and
745 Riipinen, I.: Microphysical explanation of the RH-dependent water affinity of biogenic organic aerosol and its importance
746 for climate, Geophysical Research Letters, 44, 5167-5177, 10.1002/2017gl073056, 2017.
747 Rose, D., Nowak, A., Achtert, P., Wiedensohler, A., Hu, M., Shao, M., Zhang, Y., Andreae, M. O., and Pöschl, U.: Cloud
748 condensation nuclei in polluted air and biomass burning smoke near the mega-city Guangzhou, China – Part 1: Size-
749 resolved measurements and implications for the modeling of aerosol particle hygroscopicity and CCN activity, Atmos.
750 Chem. Phys., 10, 3365-3383, 10.5194/acp-10-3365-2010, 2010.
751 Shao, L., Li, W., Yang, S., Shi, Z., and Lü, S.: Mineralogical characteristics of airborne particles collected in Beijing during a
752 severe Asian dust storm period in spring 2002, Science in China Series D: Earth Sciences $V 50, 953-959, 2007.
753 Sherman, J. P., Sheridan, P. J., Ogren, J. A., Andrews, E., Hageman, D., Schmeisser, L., Jefferson, A., and Sharma, S.: A multi-
754 year study of lower tropospheric aerosol variability and systematic relationships from four North American regions, Atmos.
755 Chem. Phys., 15, 12487-12517, 10.5194/acp-15-12487-2015, 2015.
756 Thalman, R., de Sá, S. S., Palm, B. B., Barbosa, H. M. J., Pöhlker, M. L., Alexander, M. L., Brito, J., Carbone, S., Castillo, P.,
757 Day, D. A., Kuang, C., Manzi, A., Ng, N. L., Sedlacek Iii, A. J., Souza, R., Springston, S., Watson, T., Pöhlker, C., Pöschl, U.,
758 Andreae, M. O., Artaxo, P., Jimenez, J. L., Martin, S. T., and Wang, J.: CCN activity and organic hygroscopicity of aerosols
759 downwind of an urban region in central Amazonia: seasonal and diel variations and impact of anthropogenic emissions,
760 Atmospheric Chemistry and Physics, 17, 11779-11801, 10.5194/acp-17-11779-2017, 2017.
761 Titos, G., Cazorla, A., Zieger, P., Andrews, E., Lyamani, H., Granados-Muñoz, M. J., Olmo, F. J., and Alados-Arboledas, L.:
762 Effect of hygroscopic growth on the aerosol light-scattering coefficient: A review of measurements, techniques and error
763 sources, Atmospheric Environment, 141, 494-507, https://doi.org/10.1016/j.atmosenv.2016.07.021, 2016.
764 Ulbrich, I. M., Canagaratna, M. R., Zhang, Q., Worsnop, D. R., and Jimenez, J. L.: Interpretation of organic components
765 from Positive Matrix Factorization of aerosol mass spectrometric data, Atmos. Chem. Phys., 9, 2891-2918, 10.5194/acp-
766 9-2891-2009, 2009.
767 Wiedensohler, A., Birmili, W., Nowak, A., Sonntag, A., Weinhold, K., Merkel, M., Wehner, B., Tuch, T., Pfeifer, S., Fiebig, M.,
768 Fjäraa, A. M., Asmi, E., Sellegri, K., Depuy, R., Venzac, H., Villani, P., Laj, P., Aalto, P., Ogren, J. A., Swietlicki, E., Williams, P.,
769 Roldin, P., Quincey, P., Hüglin, C., Fierz-Schmidhauser, R., Gysel, M., Weingartner, E., Riccobono, F., Santos, S., Grüning, C.,
770 Faloon, K., Beddows, D., Harrison, R., Monahan, C., Jennings, S. G., O'Dowd, C. D., Marinoni, A., Horn, H. G., Keck, L., Jiang,
771 J., Scheckman, J., McMurry, P. H., Deng, Z., Zhao, C. S., Moerman, M., Henzing, B., de Leeuw, G., Löschau, G., and Bastian,
772 S.: Mobility particle size spectrometers: harmonization of technical standards and data structure to facilitate high quality
773 long-term observations of atmospheric particle number size distributions, Atmos. Meas. Tech., 5, 657-685, 10.5194/amt-
774 5-657-2012, 2012.

https://doi.org/10.5194/acp-2019-633
Preprint. Discussion started: 30 September 2019

Atmospheric Chemistry and Physics Discussions

775 Williams, B. J., Goldstein, A. H., Kreisberg, N. M., Hering, S. V., Worsnop, D. R., Ulbrich, I. M., Docherty, K. S., and Jimenez,
776 J. L.: Major components of atmospheric organic aerosol in southern California as determined by hourly measurements of
777 source marker compounds, Atmos. Chem. Phys., 10, 11577-11603, 10.5194/acp-10-11577-2010, 2010.
778 Wu, Z. J., Poulain, L., Henning, S., Dieckmann, K., Birmili, W., Merkel, M., van Pinxteren, D., Spindler, G., Müller, K.,
779 Stratmann, F., Herrmann, H., and Wiedensohler, A.: Relating particle hygroscopicity and CCN activity to chemical
780 composition during the HCCT-2010 field campaign, Atmos. Chem. Phys., 13, 7983-7996, 10.5194/acp-13-7983-2013, 2013.
781 Wu, Z. J., Zheng, J., Shang, D. J., Du, Z. F., Wu, Y. S., Zeng, L. M., Wiedensohler, A., and Hu, M.: Particle hygroscopicity and
782 its link to chemical composition in the urban atmosphere of Beijing, China, during summertime, Atmos. Chem. Phys., 16,
783 1123-1138, 10.5194/acp-16-1123-2016, 2016.
784 Xu, W., Croteau, P., Williams, L., Canagaratna, M., Onasch, T., Cross, E., Zhang, X., Robinson, W., Worsnop, D., and Jayne,
785 J.: Laboratory characterization of an aerosol chemical speciation monitor with PM2.5 measurement capability, Aerosol
786 Science and Technology, 51, 69-83, 10.1080/02786826.2016.1241859, 2017.
787 Zhang, F., Li, Y., Li, Z., Sun, L., Li, R., Zhao, C., Wang, P., Sun, Y., Liu, X., Li, J., Li, P., Ren, G., and Fan, T.: Aerosol hygroscopicity
788 and cloud condensation nuclei activity during the AC3Exp campaign: implications for cloud condensation nuclei
789 parameterization, Atmos. Chem. Phys., 14, 13423-13437, 10.5194/acp-14-13423-2014, 2014.
790 Zhang, Q., Jimenez, J. L., Canagaratna, M. R., Ulbrich, I. M., Ng, N. L., Worsnop, D. R., and Sun, Y.: Understanding
791 atmospheric organic aerosols via factor analysis of aerosol mass spectrometry: a review, Analytical and Bioanalytical
792 Chemistry, 401, 3045-3067, 10.1007/s00216-011-5355-y, 2011.

793
794